SUBSURFACE STRUCTURAL CHARACTERIZATION, USING 2D ELECTRICAL RESISTIVITY TOMOGRAPHY AT NATIONAL ANIMAL PRODUCTION RESEARCH INSTITUTE (NAPRI), ZARIA, NIGERIA.

BY

ADAMU, JOHN
M.Sc./SCIE/10700/07-08

DEPARTMENT OF PHYSICS
AHMADU BELLO UNIVERSITY

A THESIS SUBMITTED TO THE POSTGRADUATE SCHOOL, AHMADU BELLO UNIVERSITY, ZARIA

IN PARTIAL FULFILLMENT FOR THE AWARD OF THE DEGREE OF MASTERS OF SCIENCE IN APPLIED GEOPHYSICS.

DEPARTMENT OF PHYSICS
FACULTY OF SCIENCE
AHMADU BELLO UNIVERSITY, ZARIA

OCTOBER, 2012

DECLARATION

I hereby declare that, this thesis is an original work carried out by me under the supervision of **Dr. P. O. Sule** and **Dr. K. M. Lawal**.

To the best of my knowledge, no part thereof has been submitted elsewhere for the award of degree.

The works of others are duly acknowledged and referenced.

_____	_____	_____
Name of student Author	Signature	Date

DEDICATION

I dedicate this thesis to the Almighty God whose grace was sufficient for me throughout the period of my study.

CERTIFICATION

This thesis entitled: "SUBSURFACE STRUCTURAL CHARACTERIZATION USING 2D ELECTRICAL TOMOGRAPHY AT NATIONAL ANIMAL PRODUCTION RESEARCH INSTITUTE (NAPRI), ZARIA, NIGERIA" by Adamu John, meets the regulations governing the award of the degree of Masters of Science (Applied Geophysics) of Ahmadu Bello University, Zaria and is approved for its contribution to knowledge and literary presentation.

_____ Date_____

Dr. P. O. Sule
Chairman, Supervisory Committee

_____ Date_____

Dr. K. M. Lawal
Member, Supervisory Committee

_____ Date_____

Dr. U. Sadiq
Head of Department of Physics

_____ Date_____

Prof. A. A. Joshua
Dean, Postgraduate School

ACKNOWLEDGEMENT

First and foremost, I would like to give all the glory to God almighty that stood by me in time of trials and difficulties to see that this work really succeeded, and for the good health and guidance He granted me throughout the programme.

I would like to acknowledge the assistance of the following people who have contributed in one way or the other to the success of this work.

My special thanks go to my incomparable supervisor Dr. P. O. Sule, who thoroughly supervised this work and who always had time for me to give me some corrections I needed. I am very grateful to him.

I am highly indebted to Prof. I. B. Osazuwa, who supervised the fieldwork and gave me all the necessary assistance without which this work would not have seen the light of the day. He made the equipment available for the data collection and also provided every material needed for the processing of the data. Sir, I am very grateful for your intellectual guidance. I cannot thank you enough.

I wish to also express my profound gratitude to my second supervisor Dr. K. M. Lawal, who was not bored by my persistent questions on the principle of Tomography, for his useful advice that led to the success of this work.

I owe my unreserved gratitude to Dr. Chiemeke Collins who selflessly took me to field and gave me all the technical assistance needed in the field and also during the course of data interpretation.

I cannot forget the contribution of my friend Jatto Solomon Sunday, who made his car available for me throughout the period of the field work and Mrs. Ayuba Grace Mamman for her moral support. I cannot list everyone here, but all I can say is God bless you all.

I cannot forget to mention my pastor (Revd Kehinde Olaleye) who encouraged me to embark on an M.Sc. programme; it is only God that will reward you.

I would like to acknowledge my in-law (Mr. Gideon Alabi), Dn. Isaah Adeleke, Dn. Moses Ayangbayi and his wife for their immense contribution to the success of my Masters' programme. I say thank you all.

I appreciate the contribution made by my parents Mr. and Mrs. Motunrayo Adegoke; I am going to make you people proud any time, any day.

I will not forget the sacrifice made by my brothers and sisters to see that my second degree becomes a reality. I assure you people that, in the sun or in the rain, I am with you people to the end.

ABSTRACT

The method adopted for this research work was the 2D Electrical Resistivity Tomography (ERT), using the ABEM LUND Imaging System. A Wenner configuration was carried out to map the electrical properties as an aid to characterizing the subsurface conditions. Eight profiles were occupied in the study area. For each profile, the layout geometry for the electrical imaging was such that two reels of cables were laid collinearly with 5m intervals between the takeout electrodes. Each reel had 20 takeout electrodes. However, the two innermost electrodes of the two reels of cables were connected together thus yielding effectively 41 electrodes and a spread length of 200m. The data obtained using ABEM Terrameter SAS4000 with electrode selector were processed using RES2DINV software. From the interpretation of the electrical images obtained in the study area, the depth to the fresh basement is generally well beyond 29.3m. The study reveals the presence of two distinct layers; the topsoil and the weathered basement with resistivity ranges of 20-400Ωm and 30-470Ωm respectively. These two layers constitute the overburden with a minimum thickness of 29.3m as revealed by the pseudosections. This is the maximum depth of probing achieved in the present study. The topsoil, composed of laterite and brownish sandy clay, has a thickness of about 5.0m to 7.0m. The weathered basement underlies the topsoil with a thickness of about 22.3m to 24.3m and this is the good aquifer in the study area. This layer has a relatively low resistivity due to the presence of water. The layer is highly weathered and the degree of weathering increases towards the fresh basement. This increased thickness of bedrock weathering is a proof of the capability of this layer to provide a good water reservoir with a high probability of the presence of fractures in the weathered basement. The maximum depth of probing achieved in the present study is 29.3m; this is less than the depth to the fresh basement. Hence, there is no information about the fresh basement.

TABLE OF CONTENTS

Title Page……i

Declaration……..……..ii

Dedication……..……..iii

Certification……..……iv

Acknowledgement……...……...v

Abstract..……..……..……vii

Table of Contents…….....…....….viii

List of Tables…….…….…..xi

List of Figures……...……xii

CHAPTER ONE:
GENERAL OVERVIEW

1.1 Introduction……..……..……..……..……..…1

1.2 The Survey Area……..……...……3

1.3 Location and Accessibility of the Study Area……...…6

1.4 Climate and Vegetation……...……..6

1.5 Review of Previous Study……..……...……6

1.6 Justification of the Research……...……...8

1.7 Aim and Objectives of the Survey……..……..……..……9

1.8 Scope and Limitations of the Survey…….....……10

1.9 Choice of the Method…….....……10

1.10 Importance and Uses of Electrical Imaging……..……..……...……11

CHAPTER TWO:
GENERAL GEOLOGY OF THE STUDY AREA

2.1 Introduction……...……..13

2.2 Geological Setting of NAPRI, Shika……...……..……..……13

2.3 Petrology of Shika…….……....……...15

2.3.1 Older Metasediments…….....……16

2.3.2 Younger Metasediments……...……...……16

2.3.3 Older Granite……...……...…….16

2.3.4 Younger Granite……...……..…….17

2.3.5 Gneiss……..……..…..17
2.3.6 Schist……...……..…17
2.4 Basement……...…….……18
2.5 Hydrogeology……...……...18
2.6 The Storage Element for Groundwater in Shika……...……..19
2.6.1 The Weathered Basement……...……20
2.6.2 The Laterite (Older Laterite) Deposits……..……...……20
2.6.3 The Alluvial Deposits……...……...……20

CHAPTER THREE:
PRINCIPLES AND THEORY OF THE METHOD USED

3.1 Introduction……...……21
3.2 Electrical Resistivity Method……...……...……....24
3.2.1 Vertical Electrical Sounding (VES)……...……...……24
3.2.2 Constant Separation Traversing (CST)……...……...……..26
3.3 Theory……...……...……..27
3.4 The Concept of Apparent Resistivity……...……...…….32
3.5 Limitations of Electrical Resistivity Method……...……33
3.6 Factors Affecting Electrical Resistivity of earth materials……...……...…….34
3.6.1 Water Salinity……..34
3.6.2 Porosity of Rock and effects of rock texture……..……..……35
3.6.3 Effect of Temperature……....……...……...……36
3.6.4 Effects of Geological Processes……...……...……37
3.6.5 Effects of Rock Type ……..……...……37
3.7 Reconnaissance Survey……...…….41
3.8 Instrumentation and Field Procedure…….41
3.9 Electrode Arrays……45
3.9.1 Wenner Array……...……..…….45
3.9.2 Dipole-Dipole Array……...……46
3.9.3 Wenner-Schlumberger Array……...……...…….48
3.9.4 Pole-Pole Array……..……....49
3.9.5 Pole-Dipole Array……...……..……..50

3.10 The Measurement Procedure for Wenner Electrode Configuration……...……..….51

CHAPTER FOUR:
FIELD RESULTS AND INTERPRETATION

4.1 Introduction……...……..54
4.2 Data Processing……..…….……54
4.3 Interpretation Technique……..……...……59
4.4 Geologic Section from Borehole Data……..…..……..……...…….....60
4.5 Typical Resistivity Values from previous Works……..……...……..63
4.6 Interpretation of the Results……..……..65
4.6.1 Profile One……..……...……...……65
4.6.2 Profile Two…..……...……...……...……67
4.6.3 Profile Three…..……...……...……...……..69
4.6.4 Profile Four……..……...……...……...……71
4.6.5 Profile Five…..……...……..……..…….73
4.6.6 Profile Six……...……..……...……...75
4.6.7 Profile Seven...……..……...……...77
4.6.8 Profile Eight……...……...……..……79
4.7 General Interpretation of the Results……..81
4.7.1 Variation in thickness of the Weathered Basement…….81
4.7.2 Isoresistivity Map……...…….81

CHAPTER FIVE:
DISCUSSION OF RESULTS, CONCLUSIONS AND RECOMMENDATIONS

5.1 Discussion of Results……...……...……..…84
5.1.1 Basement……...……...……84
5.1.2 Groundwater Potentials……..……85
5.1.3 Subsurface Engineering Evaluation of the Study Area……..……86
5.2 Conclusions……..……...……87
5.3 Recommendations……..……...……..89
References……....……....……..90

LIST OF TABLES

Table	Title	Page
1.1	Applicability of different electrical geophysical methods……...……....…	12
3.1	Electrical resistivity of some kinds of natural waters (ABEM Instructional Manual, LUND Imaging System)…….……...……	40
4.1	Typical Resistivity Values compiled from previous works…….……..…	62
4.2	Resistivity values Adopted for this work……...……..……..…	62

LIST OF FIGURES

Figure **Title** **Page**

1.1 Location Map Showing the Study Area……4

1.2 Google Earth Map of NAPRI Area Showing the Profile Layout around Administrative Block……5

2.1 Simplified Geological Map of Nigeria……14

3.1 An example of a Wenner Pseudo-section……23

3.2 A Sketch Showing the Principle of DC Resistivity Measurement……25

3.3 An Electrode Configuration……30

3.4 A typical range of resistivities of geological materials (ABEM Instruction Manual, 2006)……38

3.5 Figure 3.5. Picture of ABEM Lund Terrameter……42

3.6 Typical Electrode Layout of WEN32SX: Wenner CVES with two cables using the Terrameter SAS 4000 and ES464 in LUND Imaging……42

3.7 Common Arrays used in Resistivity Surveys and their Geometric Factors……44

3.8 Principle for Building up a Pseudosection……47

4.1 Arrangement of the blocks used in a model together with the Datum points in the pseudosection (RES2DINV ver 3.4)……58

4.2 Geological Well-Log obtained by Belmont Nigeria Limited……62

4.3 Electrical image along profile 1, (a) is observed data plotted as a coloured pseudosection; Ps.Z=pseudo-depth, (b) is the pseudosection computed from the model and (c) is the image or model showing true depth and true formation resistivity. ……66

4.4 Electrical image along profile 2, (a) is observed data plotted as a coloured pseudosection; Ps.Z=pseudo-depth, (b) is the pseudosection computed from the model and (c) is the image or model showing true depth and true formation resistivity. ……68

4.5 Electrical image along profile 3, (a) is observed data plotted as a coloured pseudosection; Ps.Z=pseudo-depth, (b) is the pseudosection computed From the model and (c) is the image or model showing true depth and true formation resistivity. ……70

4.6 Electrical image along profile 4. (a) is observed data plotted as a coloured pseudosection; Ps.Z=pseudo-depth, (b) is the pseudosection computed from the model and (c) is the image or model showing true depth and true formation resistivity. ……..……...…72

4.7 Electrical image along profile 5, (a) is observed data plotted as a coloured pseudosection; Ps.Z=pseudo-depth, (b) is the pseudosection computed from the model and (c) is the image or model showing true depth and true formation resistivity. ……..……...…74

4.8 Electrical image along profile 6, (a) is observed data plotted as a coloured pseudosection; Ps.Z=pseudo-depth, (b) is the pseudosection computed from the model and (c) is the image or model showing true depth and true formation resistivity. ……..……...……76

4.9 Electrical image along profile 7, (a) is observed data plotted as a coloured pseudosection; Ps.Z=pseudo-depth, (b) is the pseudosection computed from the model and (c) is the image or model showing true depth and true formation resistivity. ……..……...……78

4.10 Electrical image along profile 8, (a) is observed data plotted as a coloured pseudosection; Ps.Z=pseudo-depth, (b) is the pseudosection computed from the model and (c) is the image or model showing true depth and true formation resistivity. ……..……..……80

4.11 Surface Plot of the Weathered Basement Map of the Research Area……..…82

4.12 Isoresistivity Map of the Research Area……...…82

CHAPTER ONE

GENERAL OVERVIEW

1.1 INTRODUCTION

A geophysical investigation of the earth involves the study of physical properties, of the ground, thereby providing vital information on subsurface material conditions. This is used for numerous practical applications. The measurements are taken at or near the earth's surface that are influenced by the internal distribution of physical properties.

Consequently, analysis of these measurements can reveal how the physical properties of the earth's interior vary vertically and laterally and reflecting the subsurface geology. Alternatively, another method of investigating subsurface geology is by drilling and pitting which provide information only at discrete locations and are expensive. Many geophysical investigations are non-intrusive and non-invasive, thus avoiding the disruption caused by intrusive investigations such as drilling and pitting. Geophysical investigations cover large site areas rapidly and optimize the targeting of necessary intrusive inspections. In environments where intrusive investigations are not permissible, only geophysics is the answer. The methods employed are gravity, magnetics, seismic, electrical, radiometrics, ground penetrating radar, electromagnetic methods, etc. The methods are cost effective and capable of detecting and delineating local features of interest. For instance for groundwater exploration, electrical resistivity and seismic methods are most appropriate while gravity is a subsidiary method to the two (Kearey and Brooks, 1988).

Pressure on natural resources from growing populations, with increasing demand for water supply, infrastructure and housing, has increased over the past decades and can be expected to rise continually. Further stress on the environment due to pollution will increase the need for detailed geological knowledge, for geotechnical, hydrogeological and environmental

protection purposes. Geophysical methods can play an important role in the acquisition of such knowledge. However, the complete survey procedure, including data acquisition, data processing, interpretation and presentation must be efficient in terms of time, cost and manpower. It is also essential to ensure a continuous cover, along transects or over an area to complement point information obtained from traditional methods such as drilling, test pits, mechanical sounding, etc. This implies that at least two-dimensional (2D) information is required, and a number of 2D sections may be combined to build a 3D picture.

The method adopted for this research thesis was the 2D Electrical Resistivity Tomography (ERT), using the ABEM LUND Imaging System. A Wenner configuration and protocol WEN32SX was carried out to map the electrical properties as an aid to characterizing the subsurface conditions. Resistivity surveys determine the variation in the electrical resistivity of the subsurface by applying electric current across arrays of surface electrodes (Loke, 1999). Electrical resistivity is a function of porosity, fluid saturation, resistivity of the pore fluid and the solid, and the material texture among others. The survey data are processed to produce graphic depth sections of the thickness and resistivity of the subsurface electrical layers. The resistivity sections are correlated with ground interfaces such as soils and fill layers or soil-bedrock interfaces to provide engineers with detailed information on subsurface ground conditions. Resistivity imaging is particularly useful in clayey ground where methods such as the ground penetrating radar GPR are less effective and helps define translational boundaries that are difficult to detect using other geophysical methods (Loke, 1999).

One of the new developments in recent years is the use of 2D electrical imaging/tomography survey to map areas with moderately complex geology (Griffiths and Barker, 1993). Such surveys are usually carried out using a large number of electrodes, (25 or more), connected to a multi-core cable. In this present survey, the Wenner array with 5m

interval between 41 electrodes has been employed with each spread having a length of 200m. Eight profiles have been used. The ABEM LUND Imaging System is a multi-electrode system for cost effective and high-resolution 2D and 3D resistivity surveys, has been used for the data recording. The included data acquisition software supports 2D and 3D surveys with surface arrays which may also be used for borehole measurements. The results of analyzing the 2D Wenner resistivity sections based on 2D inversion of field data and borehole information are interpreted and presented.

1.2 THE SURVEY AREA

Shika in Zaria is situated within the northern Nigerian Basement Complex, (figure 1.1). It lies between latitudes $11^0$12'4.6"N and $11^0$12'10.2"N and longitudes $7^0$33'50.2"E and $7^0$33'64.5"E within the Zaria sheet 102. The mean elevation of the area is about 700m above mean sea level. Figure 1.2 is the National Animal Production Research Institute (NAPRI), location map showing the investigated site. The study area (NAPRI) is located inside Shika, where the profiles are laid, is bounded by latitude $11^0$12'16.1"N to latitude $11^0$12'23.8"N and longitude $7^0$33'37.6"E to longitude $7^0$33'48.6"E, with an average elevation of 683m above sea level.

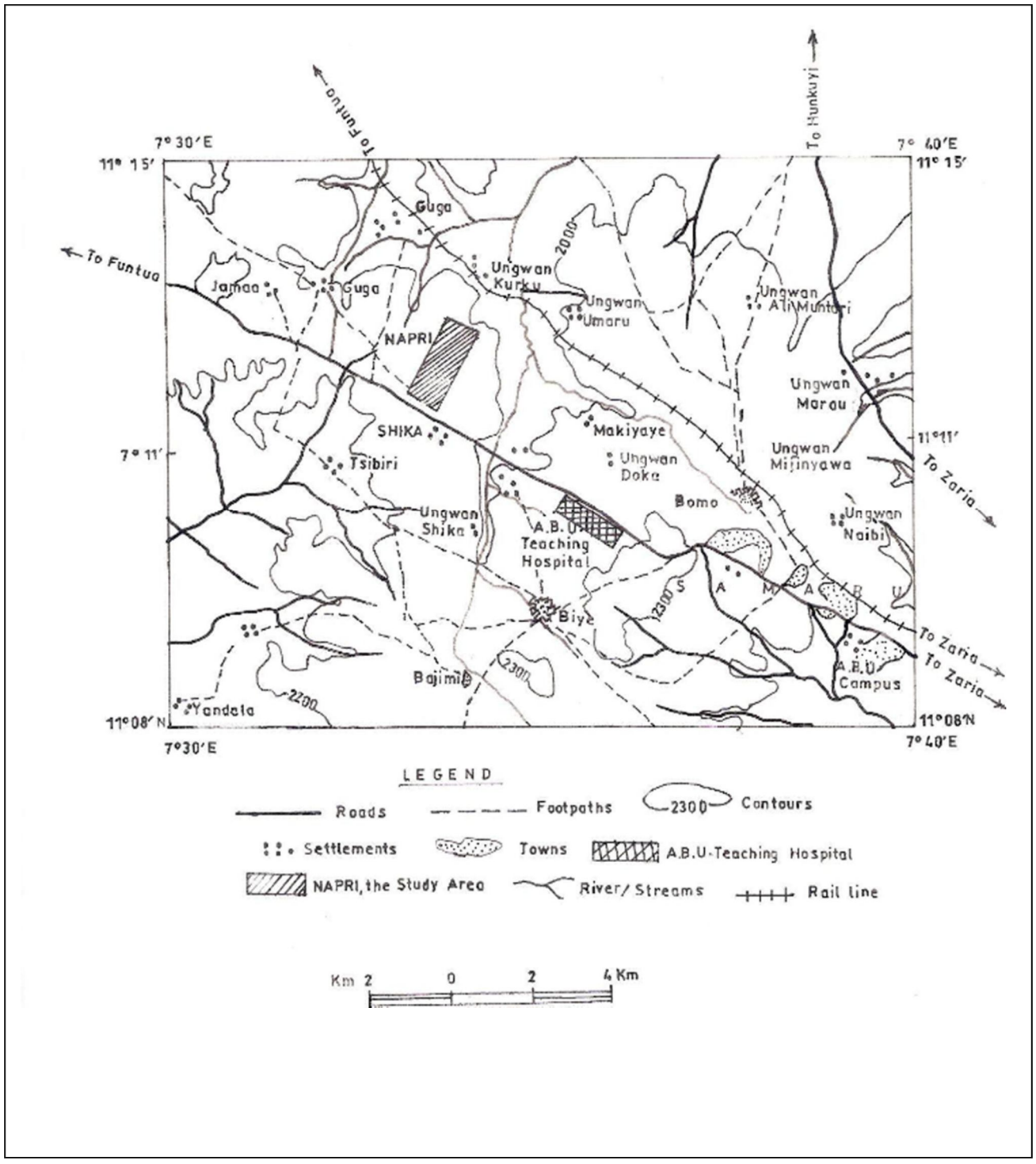


Figure 1.1 Map of Zaria showing the Study Area (Part of Zaria Sheet 102)

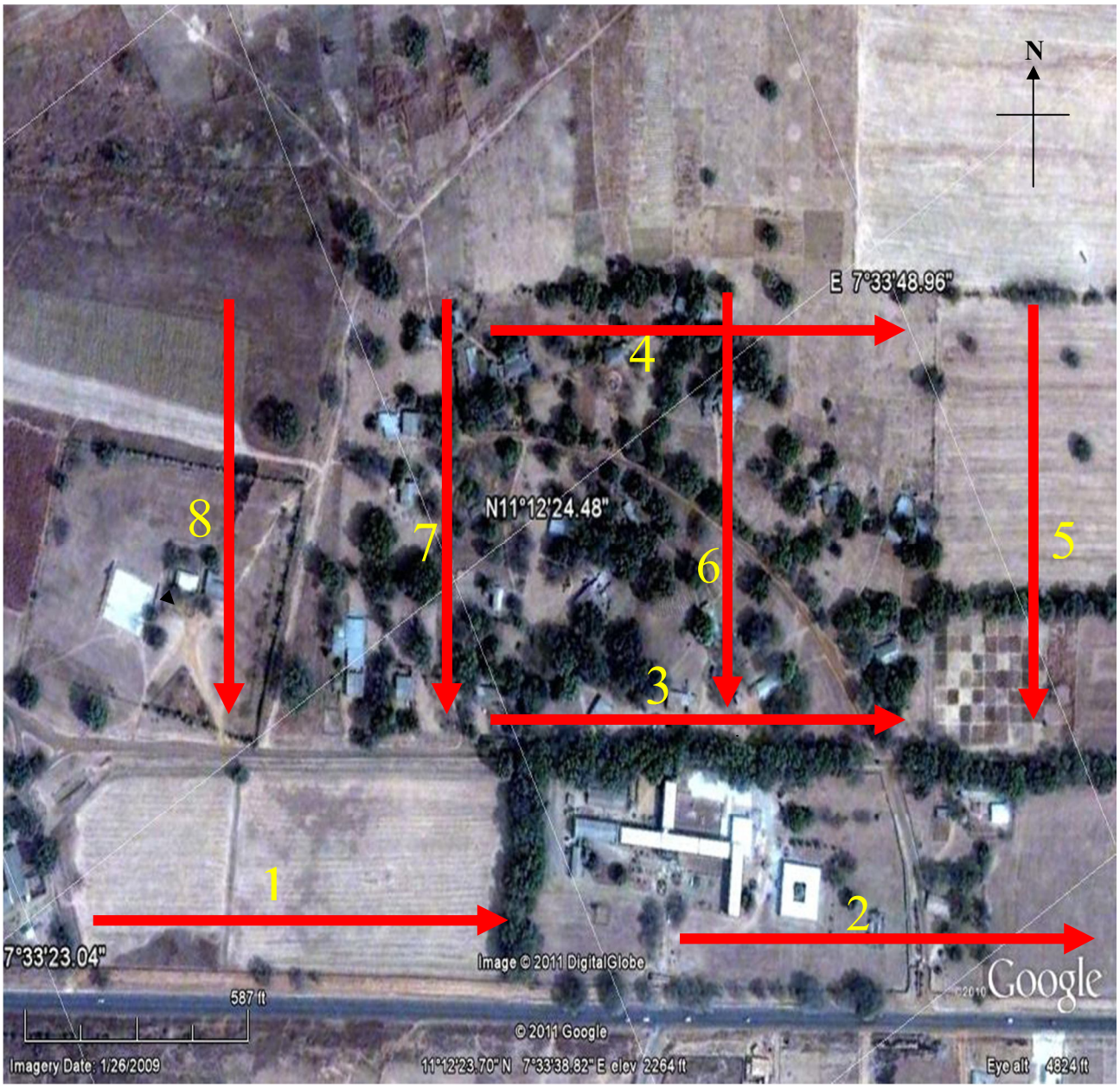


Figure 1.2 Google Earth Map of NAPRI Area Showing the Profile Layout (1-8) around Administrative Block

→ The Arrow is showing the direction of the Profile

1.3 LOCATION AND ACCESSIBILITY OF THE STUDY AREA

The National Animal Production Research Institute (NAPRI) is located in Shika, along Zaria-Funtua-Sokoto road north of Ahmadu Bello University main campus. It is bordered by Institute of Agricultural Research (IAR) farm and its dam in the south east, and Shika village in the south.

Accessibility to NAPRI is only by the Zaria-Funtua-Sokoto road which is a prominent federal road. Many all season motorable roads, some of which are tarred, also exist within the premises.

1.4 CLIMATE AND VEGETATION

The area is in the Guinea Savannah climatic belt of Nigeria with distinct dry and wet seasons. The land surface is covered by vegetation which is typical of the Savannah grassland characterized by shrub bushes generally less than 3.0m high and interrupted by large isolated trees. Normally the thick vegetation cover helps to trap rainwater and prevents severe subsurface run-off which usually gives rise to high erosion and gullying. Though the vegetation is scanty, thus, permitting erosion, it is still of advantage in arresting the depletion of groundwater and reducing the rate of evapotranspiration.

1.5 REVIEW OF PREVIOUS STUDY

In the present study area (NAPRI), however, no previous geophysical work has been done. As such the present study is meant to provide some geophysical information about the subsurface structure of the place.

Osasami (1968) carried out vertical electrical soundings to investigate groundwater potential in areas around A.B.U. main campus, Samaru. He revealed in his work that the depth

to aquifer in the area varied from about 1m to about 30m. He however, could not clearly demarcate the boundary between the weathered basement and the fresh basement.

The work by Akpoborie (1972) of hydrogeological structures which control underground water in Samaru creeks showed that structures developed in rocks such as joints and fractures control the flow of groundwater into the creeks.

Baimba (1978) carried out resistivity and seismic refraction studies for groundwater exploration at Zango, Kaduna State, which lies within the area of the basement complex of the north-central Nigeria. He concluded that the basement complex generally forms poor source of groundwater since the mantle cover is often too thin to harbor large quantities of water.

Farouq (2001) showed from his geoelectric investigation of the groundwater potential in the Institute for Agricultural Research Farm, Samaru that the thickness of weathered basement around the area varied from about 3.4m to about 30.4m.

Ojo (2007) carried out a two-dimensional electrical imaging survey of the Bomo dam. His results showed that the near surface was not consolidated; the top soil was made up of laterite, clay and sandy clay, and also that the basement rock was highly fractured. He concluded that the seasonality of the dam was due to the fractured basement, weathered basement and the unconsolidated nature of the overburden.

Chiemeke and Osazuwa (2007), worked on the application of seismic refraction tomography for subsurface Imaging in Central northern Nigeria. Their results showed that seismic refraction tomography can image the subsurface to delineate the various strata within the sub-surface; the thickness of weathered basement and depth to fresh basement were determined.

1.6 JUSTIFICATION OF THE RESEARCH

The site is situated on the basement complex with variable overburden thicknesses. Owing to the nature and large size of the land, as the expansion of the Institution grows, the management will need to develop the vacant site by erecting high-rise buildings to contain the population of the staff. The need to provide information about the subsurface sequence and structural disposition necessary for foundation design necessitated a detailed geophysical investigation of the survey area.

Also, as staff, residential people and livestock's population increases, pressure will be mounted on the only existing borehole for source of water. As such, it becomes imperative to identify other viable areas suitable for siting boreholes which will act as supplement to the existing one. This no doubt will help avert acute shortage of water in the institution in the near future.

However, delineating the aquifer units viable for future groundwater abstraction alone is not on its own satisfactory. The need to ascertain the degree of the overburden protective capacity, (i.e., the capacity to sustain massive engineering structures) which overlies the aquifer units is imperative. This is because, if the degree of the overburden protective capacity is poor or weak as the case may be, then the groundwater is adjudged vulnerable to contamination which in-turn constitutes a health hazard. If potential contamination sites such as septic tanks, waste landfills, and sewage channels are not far detached from these promising areas viable for future groundwater abstraction. The need to evaluate the protective capacity of the overburden materials has arisen in order to establish the level of safety of the hydrogeologic system in the study area with a view to enhancing safety appraisal of groundwater consumptions within the NAPRI site.

Moreover, overburden corrosiveness can lead to severe corrosion failure and this is known to be associated with low resistivity. Low electrical resistivities are indicative of good electrical conducting paths arising from increased electrolytic saturation or high concentration of dissolved salts in the soil. Evaluating the corrosiveness of the subsurface materials is necessary since it will be used to make recommendations for the nature of engineering design of steel and metal structures to be used in the study area. Where the potential for corrosion is high, the construction engineers may have to consider the incorporation of corrosion prevention system in the engineering design and the use of plastic pipes instead of metallic pipes for underground piping utilities.

1.7 AIM AND OBJECTIVES OF THE SURVEY

Since electrical images provide a more detailed view (two-dimensional) of the subsurface structure, the aim of the present research is to carry out a two-dimensional electrical resistivity imaging of the research area for hydrogeological and geotechnical development.

Using the LUND Automatic Resistivity Imaging System produced by ABEM Instrument AB, the following objectives will be achieved:

1. Determination of overburden thickness
2. Determination of the thickness of weathered basement
3. Determination of the depth to aquifer
4. Identification of the weak zones that are prone to subsidence and the competent zones that can support massive engineering structures.

1.8 SCOPE AND LIMITATIONS OF THE SURVEY

This survey has covered only some parts of the National Animal Production Research Institute (NAPRI) premises in Shika, Zaria.

A total of eight profiles were carried out in this work. The practical difficulties encountered in the field are as follows:

i. Dragging long cables and a large number of electrodes over wooded terrain constituted a problem.
ii. Hardness of the ground causing difficulties in electrode-ground contact.
iii. Partial electrode-ground contact caused by inadequate moisture caused negative results.
iv. Running down of battery in the field put a stop to the day work until it is being recharged.
v. Moving the equipment from one profile location to another around stakes and wooded terrain made the work laborious.

Another limitation of surface resistivity surveying is the decreasing resolution with depth. Furthermore, for large depth penetration very large layouts are needed and the presence of conductive layers at the surface can still reduce the depth of penetration of the method.

1.9 CHOICE OF THE METHOD

It is a common expectation that in-fill sediments or fractured rocks show a low resistivity contrast with compact basement crystalline rocks and structures, such as dikes, lava dooms, *etc* (Loke, 1999). This resistivity contrast is considered to be a good target for electrical methods. The electrical resistivity tomography survey, as a non-destructive, cost effective method, has the additional advantage of rapid data collection and interpretation. Electrical resistivity imaging is valuable for investigating the NAPRI site.

1.10 IMPORTANCE AND USES OF ELECTRICAL IMAGING

Electrical resistivity tomography prospecting involves the detection of the subsurface effects produced by electrical current flow in the ground. Many electrical techniques are available because of the large variation in the conductivity of earth materials (rocks and minerals). Theoretically at least the resistivity methods are the most superior of all the electrical methods because quantitative results are obtained using a controlled source of specific dimensions (Telford *et al*., 1976). The applicability of the different electrical methods supported by the ABEM Terrameter SAS4000 is summarized in table 1.1.

Table 1.1 Applicability of different electrical geophysical methods. SP=Self Potential, VES=Vertical Electrical Sounding, Imaging=Profiling (with different electrode separations) and IP=Induced Polarization (ABEM Terrameter SAS4000/SAS1000 instruction manual 2006)

Object of Search or Investigation	**SP**	**VES**	**Imaging**	**IP**
Archeological sites			*	
Cavities in the subsurface			*	
Clays, peat and soil	*		*	
Dam safety and leakage	*		(*)	
Groundwater in sedimentary areas		*	*	
Fracture zones in rock			*	
Groundwater in crystalline rock			*	
Groundwater/clay distinction			*	*
Groundwater flow	*			
Ores in hard rock areas	*		*	*
Overburden thickness		*	*	
Pollution of soil and groundwater			*	
Salt water invasion		*	*	*
Fissures in rock			*	

CHAPTER TWO

GENERAL GEOLOGY OF THE STUDY AREA

2.1 INTRODUCTION

Nigeria lies in the Pan African mobile belt which has been affected by Pan African events through the ages of orogenic, epeirogenetic, tectonic and metamorphic cycles. The geology of Nigeria is classified into two parts, the Basement Complex and the Sedimentary basins. The National Animal Production Research Institute (NAPRI) site, Shika, lies on a plain which forms part of the vast gentle undulating plain scenery which extended almost unbroken from Sokoto and to the south part of Kaduna (Joda, 1990). The soil is ferruginous with clay (Kaolinite) and some weathered rocks present.

The study area is part of the Nigerian Basement Complex underlain by crystalline rocks, so the geology of the area is the same as that of the Nigerian Basement complex. The rocks of the Basement Complex occupy more than 50% of the total land surface of Nigeria, and accommodate the metasediments which are made up of gneisses schists and phylittes. Exposures are scanty and highly weathered. The rock types are biotites, gneisses, granite gneisses and in parts with subordinate migmatites. The contact between the gneisses and metasediments are gradational (McCurry, 1970).

2.2 GEOLOGICAL SETTING OF NAPPRI, SHIKA

Shika in Zaria is underlain by Metasediments which forms part of the Basement Complex rocks (Fig. 2.1) of Precambrian age. The rocks are mainly schists, gneisses, and quartzites. The Zaria crystalline rocks are part of the Nigerian Basement Complex. Oyewoye (1964) showed that there is structural relationship between this Basement Complex and the rest of the West African basement. This is partly due to the fact that the whole

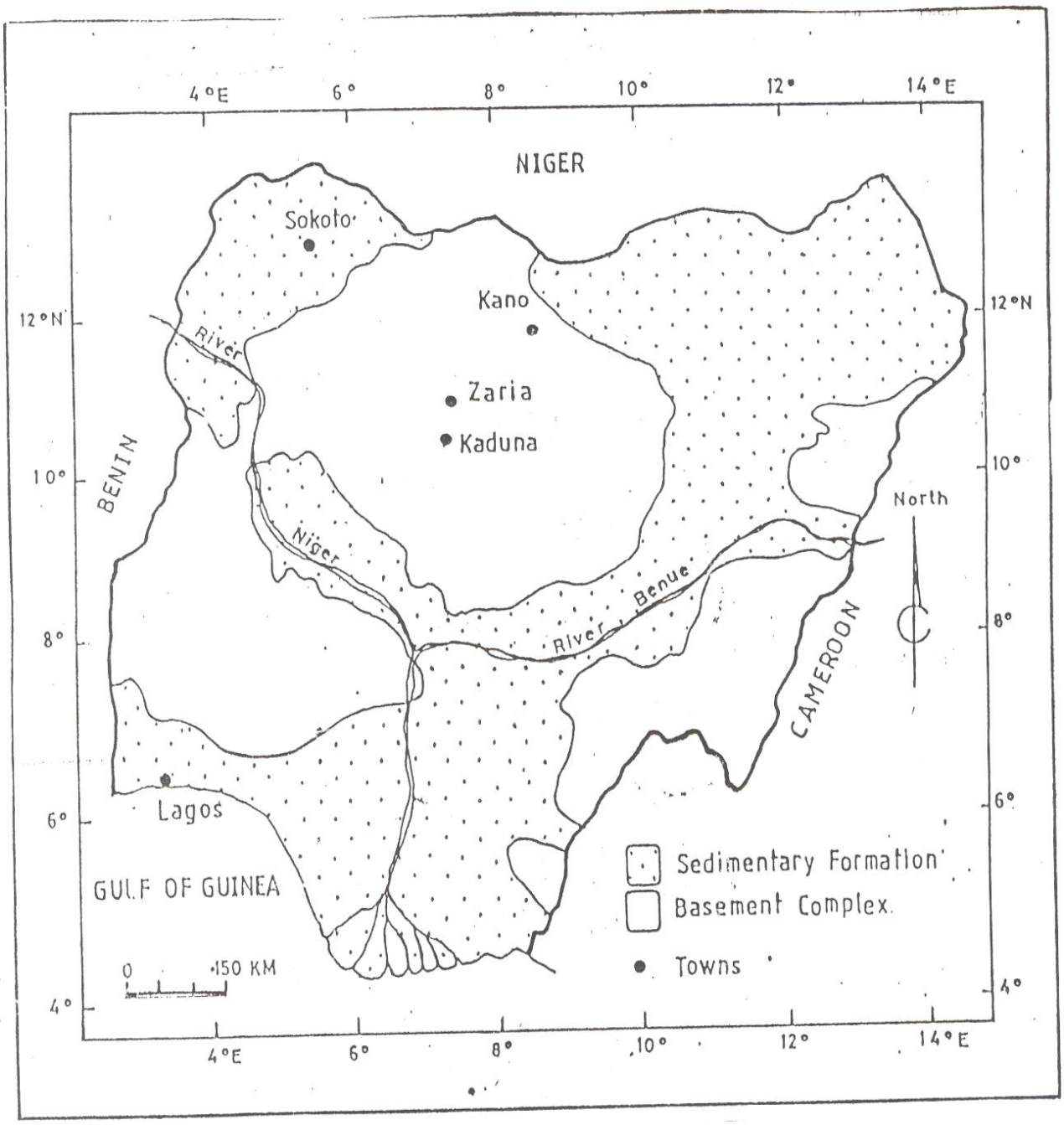


Figure 2.1 Simplified geological Map of Nigeria (Courtesy of Geological Survey of Nigeria)

region was involved in a single set of orogenic episode, the Pan African orogeny, which left an imprint of structural similarity upon the rock units.

Granitic intrusions form a suite of batholiths (the Zaria Batholiths), part of which outcrops as the Kufena Hill. The gneisses are found as small belts within the granite intrusions, and are also found east and west of the batholiths. The biotite gneiss extends westwards to form a gradational boundary with the schist belt. The gneiss continues eastwards to some extent and is occasionally broken up by the Older Granite (Wright and McCurry, 1970). The Older Granite intrusion is supposed to have been formed at the bottom of a fold mountain belt (Wright and McCurry, 1970).

The thrusting imposed on the Basement Complex during the Pan African Orogeny movement is believed to have brought together rocks of different ages with different structural and metamorphic styles (Grant, 1969). The metasediment probably belongs to the sedimentary and granite facies that were formed in a geosynclinal trough which had earlier developed at the end of the Pan African Orogeny (Tokarski, 1972). During the Pan African Orogeny, the sediments and igneous material, together with the former metamorphosed basement rocks behaved as one tectonic unit. Some of these metamorphosed rocks became assimilated into the granite intrusions that accompanied the last Orogeny (Grant, 1969).

2.3 PETROLOGY OF SHIKA

The rock types found in Shika are older granites, gneiss and migmatite; the older metasediments; and the younger metasediments and younger granites which are.discussed as follows:

2.3.1 Older Metasediments

These are believed to be Birrimian (›100 million years) in age and rock types include gneisses which have suffered at least two episodes of tectono-matemorphic deformations resulting in widespread occurrences of migmatitic and granitic gneisses (McCurry, 1976). They occupy isoclinal belts within the crystalline rocks with a N-S trending.

2.3.2 Younger Metasediments

These are found in relatively narrow well defined belts particularly in the north-west and south-west Nigeria. They are Katangan in age and believed to have been deposited on the originally granitic basement around 1800 million years ago. They were then folded during the Pan African thermotectonic events. They are found in Ilesha and occur as gold bearing quartzites in Ilorin.

2.3.3 Older Granites

They are believed to have intruded the Nigerian Basement Complex during the Eburnean and Lower Cambrian ages. The Eburnean granites are fine grained granites that represent a group of minor discordant intrusions of small aerial extent, occurring as dykes and irregular bodies. The group includes biotite and muscovite granite and adamebites. They are pale brown equigranular and usually foliated. Their contact with the later granite is complex but in some places degradational and in some places replaced by the later granite. Some of the rock types include aegerine augen granite, granodiorite granite, quartzdiorite, porphyritic biotite granite.

2.3.4 The Younger Granite

The Younger Granite series are the ring complexes of Mesozoic (Jurassic) age found in Northern Nigeria to have intruded the Precambrian to lower Palaeozoic basement rock. They are confined to a zone stretching north-south of the Jos Plateau and extend to the Niger Republic with their ages progressively decreasing from Niger republic towards Nigeria with the youngest rocks found at the southern end of the ring complex. They are a group of anorogenic rocks of Jurassic age (160 to 170 million years ago). Quite younger than the older Granite, but have equivalent composition. The major tectonic event that took place principally in the Jos Plateau around the Jurassic period resulted in the emplacement of the younger granites (Grant, 1969). Outcrops occur as large masses and sometimes as ring dykes. Members include Rhyolites, Syenites and Gabbros.

2.3.5 Gneiss

The gneissic complex is medium to coarse grained and are moderately to weakly foliated rocks. They are principally composed of quartz, oligoclase, biotite and occasionally porphyroblastic microcline (Wright and McCurry, 1970). The Older Granites are non-porphyroblastic and are variably foliated. They contain concordant biotite-rich segregation and are mainly composed of quartz, turbid oligoclase and accessory apatite (Trustwell and Cope, 1963).

2.3.6 Schist

The schist is found as parallel lenses in the biotitic gneiss west of Ungwan Kubanni, in the stream valleys. The schist occurs in thin vertical sheets striking in the north-south direction.

The schistose metasediment contains mainly biotite feldspar and quartz (Adamu, 1973). Quartzites are often associated and concordant with the schistose lenses.

2.4 BASEMENT

Basement geology was affected by an orogeny which predated the emplacement of the older granite. During this event, deformation of the basement produced north-south trending basin of metasediment in the form of synclinoria (Trustwell and Cope, 1963). Tertiary east movement tilted the metasediments to the north and warped the basement along the axis of uplift (Russ, 1957). Two of the Russ' axes pass through the present Kaduna State having north-south trend and have a pronounced effect on the drainage of the state. Crystalline rocks of the Basement complex may be altered, jointed or fractured. The process of alteration may give rise to loose aggregates above fresh basement or sometimes may create a laterite cover and a clayey horizon above loose altered bedrock. Primary porosities of fresh basement rocks are very low and most times less than 30% (Russ, 1957). The rocks have very low permeability due to the presence of a few pores that are normally interconnected. The weathered profile covering the fresh fractured basement rocks consisting of clayey and lateritic material changes down profile to fresh bedrock. This material forms the aquifer.

2.5 HYDROGEOLOGY

Hydrogeology is often influenced by the climate, structure and geology of an area. This is because the geological formations underlying the area and their structures determine the type of aquifer to be encountered and the means of recharging them. The climate determines the water content and the rate of recharge of an aquifer. The climate and hydrological conditions control the surface and subsurface water in the area. The surface water is controlled by the

underlying geology. Infiltration, evaporation, run off and overflow are the major factors responsible for groundwater recharge and accumulation (Farouq, 2001).

Rainfall is the dominant factor that determines the occurrence of groundwater in the survey area. As such, this factor greatly affects the groundwater in Shika. During the rainy season, Shika catchment's areas enjoy a fairly high amount of rainfall. Rainfall data for the last forty years show that the highest rainfall occurs in August while the lowest is in November.

The higher the precipitation over an area, the greater the recharge of the groundwater. It has been observed that wells dug away from the river normally contain water at shallow depths. However, the water table falls progressively throughout the dry season. The amount of fall is determined by the location of the well from the river (Olowu, 1967). Generally, the closer a well is to the river channel, the smaller the fall. This fall is mainly controlled by subsurface percolation of water into larger river valleys. Since the groundwater in the area is unconfined, there are seasonal fluctuations in the water table (Olowu, 1967).

2.6 THE STORAGE ELEMENT FOR GROUNDWATER IN SHIKA

The types of structures developed in the rocks also affect the occurrence of groundwater. Some rocks have porespaces which are filled with water while others have dry porespaces or none at all. In igneous rocks, porosity occurs primarily in the form of joints and fractures. Other non crystalline rocks may be naturally highly permeable. The criteria that make formation of a good aquifer include high effective porosity and permeability. These in turn depend on the degree of weathering and fracturing of the rocks.

The storage elements for groundwater in the Shika surrounding are described as follows:

2.6.1 The weathered basement

Generally in this region, the weathered basement is the most important aquifer. The thickness of this aquifer varies from place to place in the area and is covered in most places by lateritic loam (Wrights 1970; Eigbefo 1978). Wherever it is exposed to erosion, it exhibits evidence of mobilization (McCurry, 1970). Where the weathering of the rock has been in situ, which is mostly the case in this area, the weathered product is usually capped by laterite.

2.6.2 The laterite (Older Laterite) deposits

These deposits contain little water. They are mostly unconsolidated and, because they are shallow, they receive direct recharge from rainfall. They are found all around the study area. They have varying thicknesses ranging from less than 1.0m to about 10.0m in some places in the area (Wright and McCurry, 1970).

2.6.3 The alluvial deposits

These consist of gravels, sands, silts and clay deposits. They are mostly found along the river channel and have thicknesses that vary from 5m – 15m (Olowu, 1967).

CHAPTER THREE

PRINCIPLES AND THEORY OF THE METHOD USED

3.1 INTRODUUCTION

The electrical resistivity imaging is a survey technique recently developed for the investigation of areas of complex geology where the use of resistivity sounding and other techniques are unsuitable (Griffiths and Barker, 1993). It involves measuring a series of constant separation traverses with the electrode spacing being increased with each successive traverse. Since increasing separation leads to greater depth penetration, the measured apparent resistivities may be used to construct a vertical contoured section displaying the variation of resistivity both laterally and vertically over the section.

The major limitation of the resistivity sounding method is that it does not take into account horizontal changes in the subsurface resistivity. A more accurate model of the subsurface is a two-dimensional (2-D) model where the resistivity changes simultaneously in the vertical direction, as well as in the horizontal direction along the survey line. In many situations, particularly for surveys over elongated geological bodies, the imaging technique gives a clearer picture of the cross-section of the body than what the vertical electrical sounding (VES) would do. In theory a 3-D resistivity survey and interpretation model should even be more appropriate. However, at the present time, 2-D surveys are the most practical economic compromise between obtaining very accurate results and keeping the survey costs down. Typical 1-D resistivity sounding surveys usually involve about 10 to 20 readings, while 2-D imaging surveys involve about 100 to 1000 measurements. In comparison, 3-D surveys usually involve several thousand measurements.

The cost of a typical 2-D survey could be several times the cost of a 1-D sounding survey, and is probably comparable with a seismic survey. In many geological situations, 2-D

electrical imaging surveys can give useful results that are complementary to the information obtained by other geophysical methods. For example, seismic methods can map undulating interfaces well, but will have difficulty (without using advanced data processing techniques) in mapping discrete bodies such as boulders, cavities and pollution plumes. Ground radar surveys can provide more detailed pictures but have very limited depth penetration in areas with conductive unconsolidated sediments, such as clayey soils. Modern field systems, such as the Lund imaging system (Terrameter SAS 4000/1000) use a multicore cable to which 24 or more electrodes are connected at takeouts moulded on at predetermined equal intervals. Such a cable is very much like a seismic cable and is used in a similar way. The cable is connected to a switching module and to an earth resistance meter and computer through an RS232 port. With these systems, any electrodes may be switched to act as either current or potential electrodes and so within the constraints of the electrodes emplaced, any electrode arrangement can be employed. In practice either the two-electrode (pole – pole), Wenner, pole – dipole or dipole – dipole arrays are employed.

The first stage in the production of an electrical image is the construction of a pseudosection (Barker 1989, Edwards 1977). It is a common method for qualitative presentation of resistivity data.

A pseudosection is made by plotting the data points in a diagram, using the length axis for the distance along the surveying line and the depth axis for electrode separations. The distance for the electrode configuration midpoint is thus plotted against the electrode separation for each measured data point.

The corresponding apparent resistivities for the plotted points are then used to contour the variation in apparent resistivity along the surveying line. The pseudosection thus obtained reflects the variation of resistivity in the ground in a qualitative way. Figure 3.1 shows an

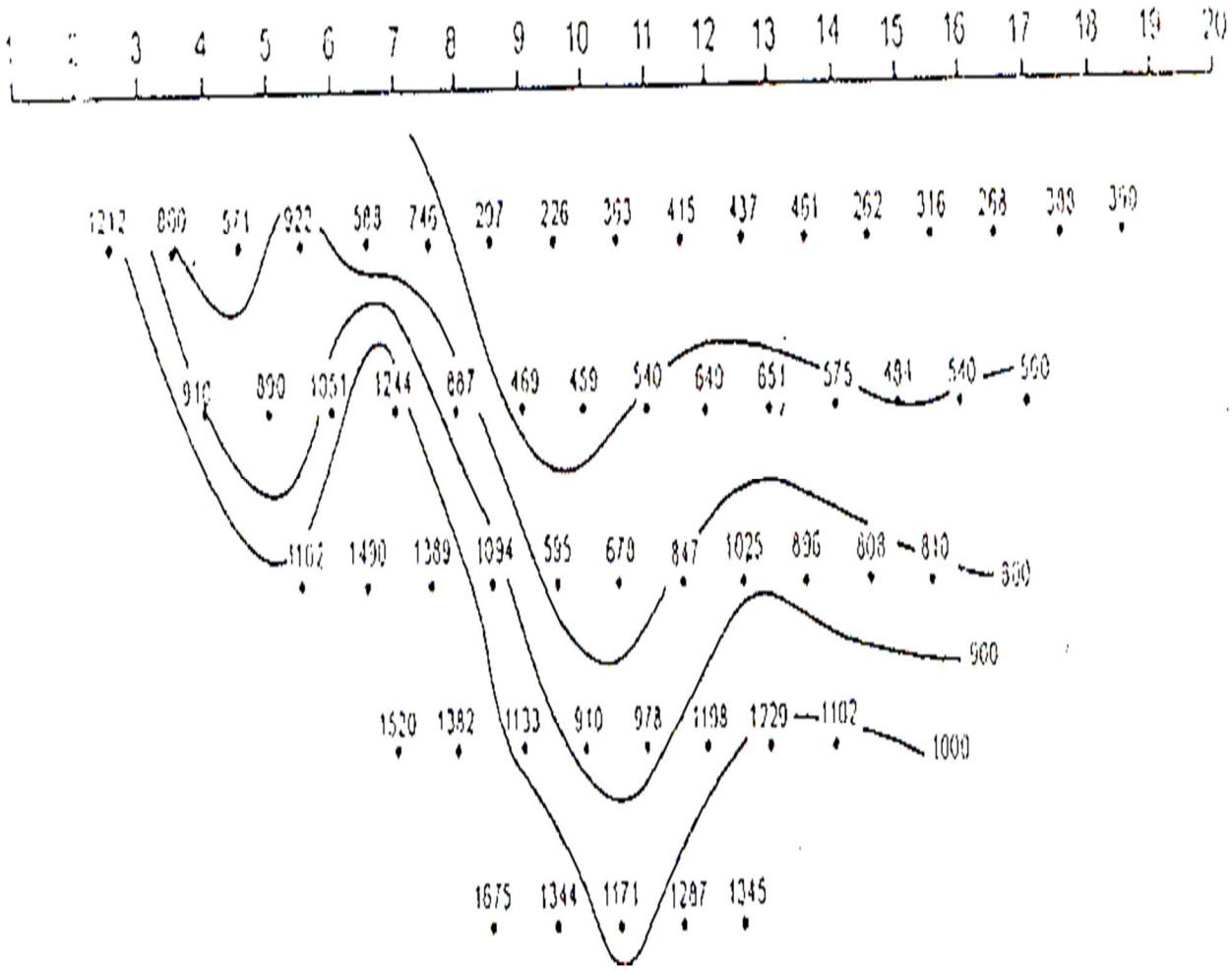


Figure 3.1 An example of a Wenner Pseudo-section (ABEM Terrameter SAS4000/ SAS1000 instruction manual, 2006)

example of a Wenner Pseudosection. Pseudosection is simply a 2D equivalent of the plotted field data points in a VES diagram.

3.2 Electrical Resistivity Method

The resistivity method is based on measuring the potentials between one electrode pair while transmitting direct current (DC) between another electrode pair (Fig. 3.2). The depth of penetration is proportional to the separation between the electrodes, in homogeneous ground, and varying the electrode separation provides information about the stratification of the ground. Interpreting the resistivity data consists of two steps: a physical interpretation of measured data, resulting in a physical model, and a geological interpretation of the resulting physical parameters.

The electrical resistivity surveys are used routinely in geothermal, mining, coal, groundwater and engineering applications (Keller and Frischknecht, 1966). In engineering application, electrical surveys are used for dam stability studies, bedrock strength, mapping overburden, faults and fracture.

There are three basic modes of operation for any resistivity method: sounding, profiling and sounding-profiling.

3.2.1 Vertical Electrical Sounding (VES)

This is also known as electrical drilling or expanding probe. It is used mainly in the study of horizontal or near–horizontal interfaces. In this method the current and potential electrodes are maintained at the same relative spacing and the whole spread is progressively expanded about a fixed central point. Consequently, readings are taken as the current reaches progressively greater depth.

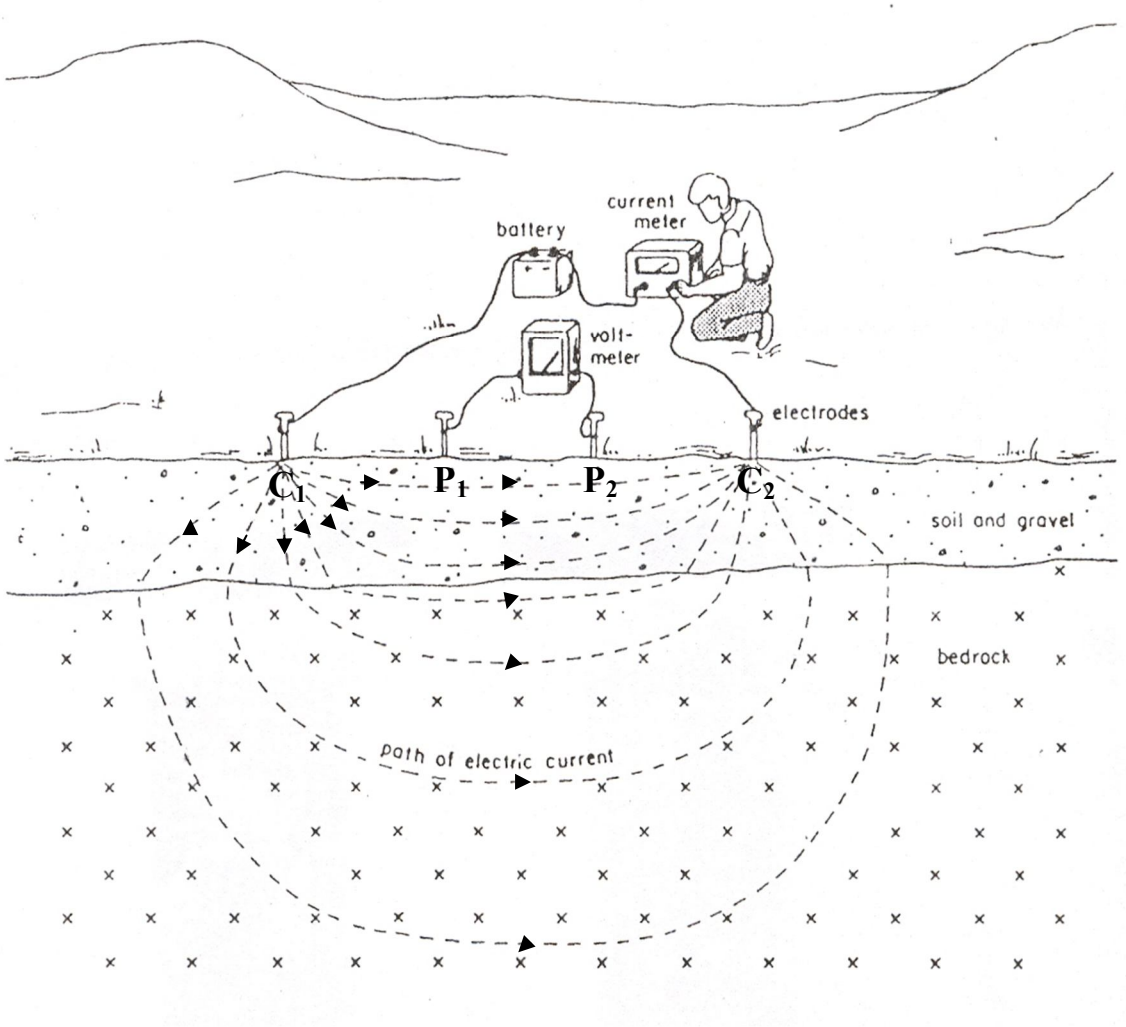


Figure 3.2. A Sketch Showing the Principle of DC Resistivity Measurement

⟶ Arrows show the direction of flow of current

The measured apparent resistivity values are normally plotted against electrode spacing values on a log–log graph paper. To interpret the data from such a survey, it is normally

assumed that the subsurface consists of horizontal layers. In this case, the subsurface resistivity changes only with depth, but does not change in the horizontal direction.

In many engineering and environmental studies, the subsurface geology is very complex where the resistivity can change rapidly over short distances. The resistivity sounding method might not be sufficiently accurate for such situations. However, the technique is extensively used in geotechnical surveys to determine overburden thickness and also in hydrogeology to define horizontal zones of porous strata.

3.2.2 Constant Separation Traversing (CST)

This is also known as electrical profiling. It is used to determine lateral variations of resistivity. The current and potential electrodes are maintained at a fixed separation and the array is progressively moved along different profiles. This gives some information about lateral changes in the subsurface resistivity, but cannot detect vertical changes in the resistivity. This method is employed in mineral prospecting to locate faults or shear zones and to detect localized bodies of anomalous conductivity. It is also used in geotechnical surveys to determine variations in bedrock depth and the presence of steep discontinuities. Results from a series of CST traverses with fixed electrode spacing can be employed in the production of resistivity contour maps.

The most useful method is a combination of sounding and profiling which delineates both lateral and vertical variations in resistivity. This is the method employed in electrical imaging.

3.3 THEORY

The principle underlying the resistivity method is embodied in Ohm's law, which states that the current density at a given point is proportional to the electric field intensity at that point. Thus, Ohm's law gives the relationship between current density J (amperes/m^2) and electric field intensity E (volts/m) as:

$$J = \sigma E \quad \text{(3.1)}$$

Where σ is the conductivity of the medium. Also E is the gradient of a scalar potential U (volts), i.e.,

$$E = -\nabla U \quad \text{(3.2)}$$

Putting equation (3.2) into equation (3.1)

$$J = -\sigma \nabla U \quad \text{(3.3)}$$

From divergence condition,

$$\nabla \cdot J = 0 \quad \text{(3.4)}$$

Thus, from equation (3.3)

$$\nabla J = -\nabla \cdot (\sigma \nabla U) = 0 \quad \text{(3.5)}$$

Or

$$\nabla \sigma \cdot \nabla U + \sigma \nabla^2 U = 0 \quad \text{(3.6)}$$

For a homogeneous earth, σ is a constant and since the derivative of a constant is equal to zero, then the first term in equation (3.6) vanishes hence,

$$\nabla^2 U = 0 \quad \text{……..}$$

(3.7)

Applying boundary conditions, equation (3.7) can be solved for specific cases. For instance, for a single current electrode at the surface of a homogeneous ground, equation (3.7) is expressed in spherical polar coordinates as:

$$\frac{1}{r^2}\frac{\partial}{\partial r}\left(r^2\frac{\partial U}{\partial r}\right)+\frac{1}{r^2\sin\theta}\frac{\partial}{\partial\theta}\left(\sin\theta\frac{\partial U}{\partial\theta}\right)+\frac{1}{r^2\sin^2\theta}\left(\frac{\partial^2 U}{\partial\phi^2}\right)=0 \text{ ----------}$$

(3.8)

For point current source, there is complete symmetry of current flow with respect to the **θ** and **ϕ** directions and the derivatives with respect to these directions are zero. Thus, equation (3.8) becomes

$$\frac{\partial}{\partial r}\left(r^2\frac{\partial U}{\partial r}\right)=0=\frac{d}{d}\left(r^2\frac{dU}{d}\right)$$

……..(3.9)

Integrating the equation twice gives

$$r^2\frac{\partial U}{\partial r}=a \qquad \text{And} \qquad U=-\frac{a}{r}+b$$

Where **a** and **b** are constant and r is the distance from the single current electrode. Since U = 0 as r $\rightarrow\infty$ then b = 0

$$U=-\frac{a}{r} \text{ ……..}$$

(3.10)

The current flows radially outwards in all direction from the point current electrode and the total current crossing a sphere of radius **r** is

$$I = 4\pi r^2 J = -4\pi r^2 \sigma \frac{dU}{dr} = 4\pi\sigma a = -\frac{4\pi a}{\rho} \quad \text{.....(3.11)}$$

Using equation (3.3) and equation (3.10)

$a = -\frac{I\rho}{4\pi}\frac{1}{r}$ So that in equation (3.10), by substitution

Hence

$$U = \frac{I\rho}{4\pi}\frac{1}{r} \qquad \text{Or} \qquad \rho = 4\pi r\left(\frac{U}{I}\right) \quad \text{.....}$$

(3.12)

The equipotentials which are everywhere perpendicular to the current flow lines will be spherical surface given by r is equal to a constant.

The point current electrode of the three-point-system is located at the surface of the homogeneous isotropic medium θ the air above having zero conductivity, the return current electrode is at a great distance. As in the previous case b=0 since U=0 as $r \to \infty$

In addition $\frac{\partial U}{\partial z} = 0$ at z = 0

Since $\sigma_{air} = 0$. In the present case, all the current flows through a hemispherical surface in the lower region.

Hence

$$a = -\frac{I\rho}{2\pi} \qquad \text{And} \qquad U = \frac{I\rho}{2\pi}\frac{1}{r} \quad \text{or} \quad \rho = 2\pi r\left(\frac{U}{I}\right) \quad \text{.....}$$

(3.13)

Thus generally, the potential difference between 2 arbitrarily located points on the surface of a homogeneous isotropic ground is given by the following expression.

$$\Delta U = \frac{I\rho}{2\pi}\left(\frac{1}{r_1}-\frac{1}{r_2}-\frac{1}{r_3}+\frac{1}{r_4}\right) \quad \text{.....}$$

(3.14)

Where ρ is the resistivity, **I** is the current and r_1, r_2, r_3, and r_4, are the inter-electrode distances as shown in Figure (3.3.)

From equation (3.11) the apparent resistivity can be solved for as;

$$\rho_a = \frac{\Delta U}{I}\frac{2\pi}{\left(\frac{1}{r_1}-\frac{1}{r_2}-\frac{1}{r_3}+\frac{1}{r_4}\right)} \quad \text{.....}$$

(3.15)

The result is independent of the position of the electrodes and is not affected when the current and the potential electrodes are interchanged.

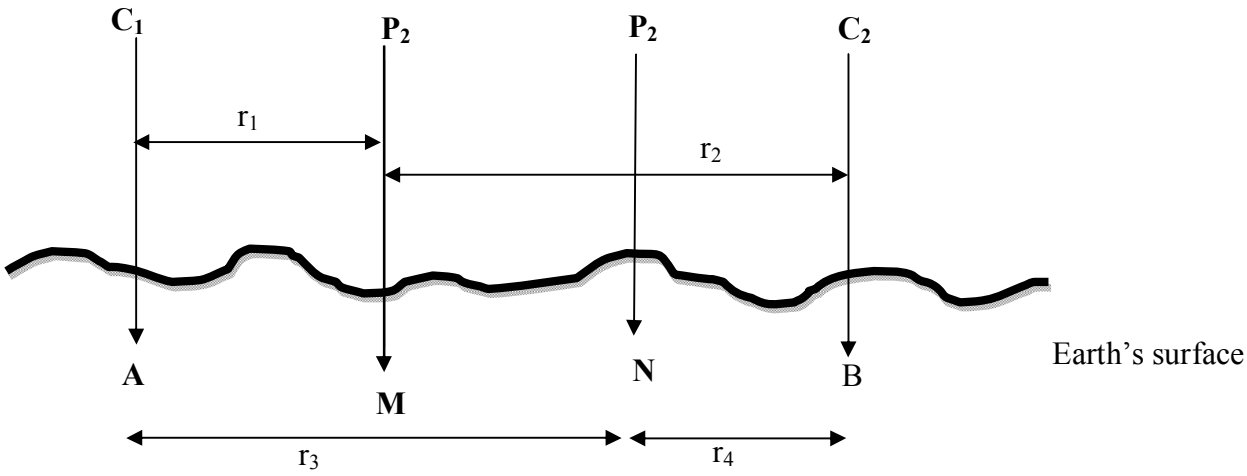


Figure 3.3 An electrode configuration

The resistance is calculated using Ohm's law:

$$R = \frac{\Delta U}{I} \quad \text{..... (3.16)}$$

Where **R** is the resistance in ohms; ΔU is the potential difference in volts; and **I** is the current in amperes.

The material parameter **ρ** which is the inverse of electrical conductivity **σ** is related to the resistance via a geometric factor **K** that is a function of the electrode configuration. The resistivity of the homogeneous ground can be calculated using, the relation

$$\rho = K \frac{\Delta U}{I} \quad \text{.....} \quad (3.17)$$

Where $K = \frac{2\pi}{\left(\frac{1}{r_1} - \frac{1}{r_2} - \frac{1}{r_3} + \frac{1}{r_4}\right)}$ ..... (3.18)

The Wenner spread (WEN32SX) CVES was adopted for this survey. Depth probes provide models of vertical variations in ground resistivity using an expanded electrode array offset from

a central reference point. Depth penetration increases with wider electrode separation providing a 2-D layered resistivity model. Composite sections are produced by interpolating between depth probes taken at regular intervals along a survey line. Resistivity imaging is an advanced development of the traditional resistivity surveying using four equally spaced electrodes set in standard Wenner configuration. Enhanced data quality and resolution provide continuous 2-D resistivity models. Forty-one electrodes were used and unit electrode spacing is determined by parameters such as profile length, desired resolution and targeted depth of penetration.

A switching unit takes a series of constant separation readings along the entire length of the electrode array. The separation between sampled electrodes is then widened to increase the effective depth penetration. Electrodes are sequentially activated as either current or potential electrodes and apparent resistivities are determined for numerous overlapping electrode configurations.

These numerous measurements along a line yield a distribution of apparent resistivities for the subsurface. The apparent resistivities are then converted to true resistivity values using a numerical inversion that determines the best least-squares fit to the observed data with an objective function smoothing term that stabilizes the inversion (Ward, 1990).

3.4 THE CONCEPT OF APPARENT RESISTIVITY

Most resistivity techniques define a response function called apparent resistivity, ρ_a which can be calculated from the surface measurements. These apparent resistivities are usually functions of a variable that is related to the depth of current penetration.

The apparent resistivity is equal to the true resistivity only when the subsurface is homogeneous. In practice, this condition is difficult to obtain. However, the subsurface is assumed to be divided into thin strata with each stratum regarded as completely homogeneous

and isotropic (Koefoed, 1979); this is a convenient way of representing a response of the actual distribution of lateral resistivity in the surface on the basis of subsurface measurements. If the electrodes are laid out along a profile and their separations are increased systematically, the change in the apparent resistivity will be a function of electrode spacing.

Subsurface resistivity is measured by applying an electric current through two current electrodes and measuring the resulting voltage difference between potential electrodes. For the general four electrode spread, the potential difference ΔU between the potential electrodes is given by (equation 3.14).

By measuring $\mathbf{\Delta U}$ and $\mathbf{I}$ and knowing the electrode configuration, the resistivity can be calculated. Over uniform earth or homogeneous isotropic medium this calculated resistivity is constant for different electrode separation and any current. However, if the ground is inhomogeneous, the calculated resistivity varies as the electrode spacing is varied or the array is moved about. This calculated resistivity is called "apparent resistivity ρ_a", which is diagnostic of the real resistivities of the subsurface in the vicinity of the electrode array. The apparent resistivity may be smaller or larger than the real resistivities or in rare cases identical with one of the real resistivity values. The apparent resistivity is the same as the real resistivity in a homogeneous subsurface, but normally a combination of contributing strata of an inhomogeneous subsurface. The value of the apparent resistivity obtained with small electrode spacing is called the surface resistivity. In any layout, the potential and current electrodes can be interchanged and from the principle of reciprocity, the apparent resistivity should be the same (unchanged) in either case.

3.5 LIMITATIONS OF ELECTRICAL RESISTIVITY METHOD

Resistivity surveying is an efficient method for delineating shallow layered sequences or vertical discontinuities involving changes of resistivity.

It does, however, suffer from a number of limitations:

(1) Interpretations are ambiguous. Consequently, independent geophysical and geological controls are necessary to discriminate between valid alternative interpretations of the resistivity data.

(2) Interpretation is limited to simple structural configuration. Any deviations from these simple situations may be impossible to interpret.

(3) Topography and the effects of near-surface resistivity variations can mask the effects of deeper variations.

(4) The depth of penetration of the method is limited by the maximum electrical power that can be introduced into the ground and by the practical difficulties of laying out long lengths of cable.

3.6 FACTORS AFFECTING ELECTRICAL RESISTIVTY OF EARTH MATERIALS

The electrical resistivity of rocks and minerals is an extremely variable property and depends on a number of factors. Bulk resistivities from the surface to more than 15km depth in a normal crust are controlled by aqueous electrolytic conduction by way of pores, fractures, faults, and shear zones. The resistivity of crystalline rock formations such as granulites, granite, and diorite in situ is largely dependent upon the water in the fissures and fractures. Similarly, the porosity, degree of saturation and the nature of pore-electrolytes govern the resistivity of rocks like sandstone and limestone. A slight increase in resistivity with depth is the result of decreasing pore, fracture, fault and shear-zone porosity due to increased lithostatic load.

3.6.1 Water Salinity

Conduction in near-surface rocks is largely electrolytic, taking place in connected pore spaces, along grain boundaries, in fractures, faults and shear zones but negligibly through the silicate framework. The ions which conduct the current result from the dissociation of salts, such dissociation occurring when salts are dissolved in water. Since each ion is able to carry only a definite quantity of charge, it follows that the more ions that are available in a solution the greater will be the charge that can be carried. Hence, a solution with a large number of ions will have a high conductivity. In general, for a given porosity, a rock which contains saline water within its pores will have a greater conductivity when the salinity of the water is high than when it is low. Resistivity decreases with increasing salinity.

3.6.2 Porosity of Rock and Effects of Rock Texture

Porosity can be defined as the ratio of the percentage of the volume of void space to the total volume of the rock. Porosity arises from the fact that the particles do not occupy all the possible space. It provides a direct measure of the total void space available for the storage of fluids (Clark, 1960).

Resistivity and porosity in sedimentary rocks can be related by the general form of Archie's law, which for rocks devoid of clay is written as

$$f = \frac{\rho_r}{\rho_s} = \alpha\phi^{-m} \quad \text{..... (3.19)}$$

where ***f*** is the formation resistivity factor**;** ρ_r is the resistivity of the rock; ρ_s is the resistivity of the solution in the pores of the rock; ϕ is porosity, while ***α*** and ***m*** are constants peculiar to the rock type. The constant ***'m'*** is usually referred to as the ***cementation factor*** while the constant ***α***

is referred to as the ***coefficient of saturation***. The most common minerals forming soils and rocks have very high resistivity in a dry condition, and the resistivity of soils and rocks is therefore normally a function of the amount and quality of water in pore spaces and fractures.

The texture of a rock dictates its resistivity in the following ways.

i. A well sorted sandstone has large void spaces and hence exhibits low resistivity.

ii. A poorly-sorted sandstone will have a much lower porosity and hence will exhibit higher resistivity.

iii. Dissolution along fractures in a limestone will enhance porosity and hence lower resistivity.

iv. Precipitation of some minerals in any rock will lower the porosity and hence increase resistivity

v. Basalt has much unconnected or dead-end pore space and hence low permeability, so that even basalt of high porosity may exhibit high resistivity.

3.6.3 Effect of Temperature

An increase in temperature lowers the viscosity of water, with the result that ions in the water become more mobile. The increased mobility of the ions results in an observed resistivity decrease with increase in temperature according to the following formula (Keller and Frischknecht, 1966).

$$\rho_t = \frac{\rho_{18}}{1+\alpha(t-18)} \quad \text{.....} \quad (3.20)$$

Where ρ_t is the resistivity at this temperature t, ρ_{18} is the resistivity at 18°C, α is the temperature coefficient of resistivity (about 0.025 per degree Celsius) and t is the ambient temperature.

3.6.4 Effects of Geological Processes

In general, geological processes reduce the resistivity of a rock but there are exceptions. Weathering of hydrothermal alteration of granite significantly lowers its resistivity. Dissolution, faulting and shearing usually increase porosity and fluid permeability, and hence lower resistivity. Precipitation of calcium carbonate and silica reduces porosity and hence reduce fluid permeability and increase resistivity. Indurations by compaction or metamorphism will reduce porosity and permeability and hence increase resistivity. Salt water intrusion provides more ions for conduction and therefore reduces resistivity.

3.6.5 Effects of Rock type

Figure 3.4 displays the typical ranges of resistivities for a number of rock and soil types. These ranges in part reflect the textural types and the effects of the geological processes. The resistivity of a type of soil and rock may vary widely. However, the variation may be more limited within a confined geological area and variations in resistivity within a certain soil or rock type will reflect variations in physical properties. For example, the lowest resistivities encountered for sandstones and limestones mean that the pore spaces in the rock are saturated with water, whereas the highest values represent strongly consolidated sedimentary rock or dry rock above the groundwater surface.

The amount of water in a material depends on the porosity, which may be divided into primary and secondary porosity. Primary porosity consists of pore spaces between the mineral

particles and occurs in soils and sedimentary rocks. Secondary porosity consists of fractures and weathered zones, and this is the most important porosity in crystalline rocks such as granites and gneisses. Secondary porosity may also be important in certain sedimentary rocks such as

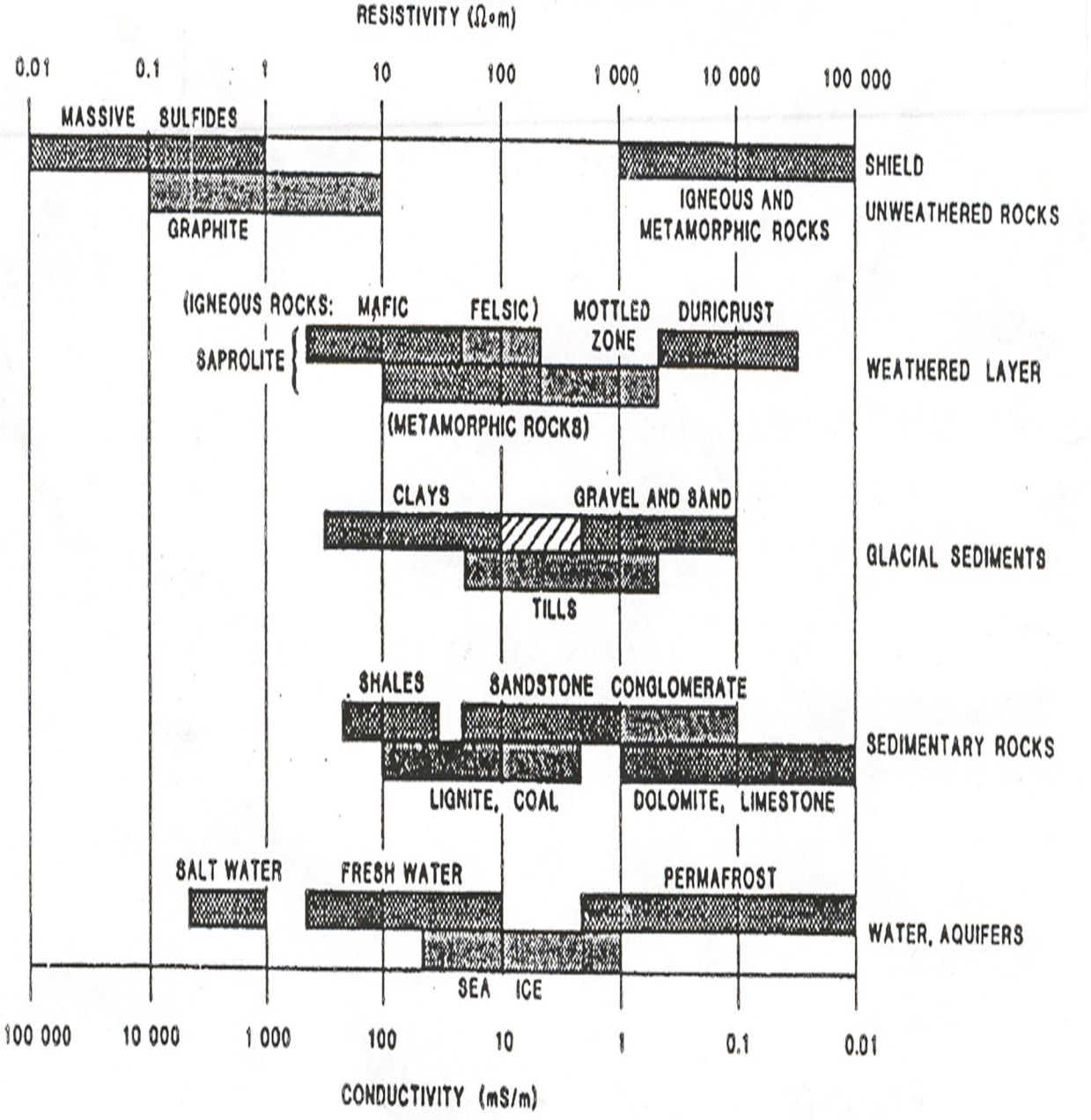


Figure 3.4 A typical range of resistivities of geological materials (ABEM Instruction Manual, 2006).

limestone. Even if the porosity is rather low, the electrical conduction taking place through water filled pore spaces may reduce the resistivity of the material drastically. The degree of water saturation will of course affect the resistivity, thus the resistivity above the groundwater level will be higher than below if the material is the same. Consequently, the resistivity can be used to find the depth to groundwater in materials where a distinct groundwater table exists. However, if the content of fine grained material is significant, the water content above the groundwater surface, held by hygroscopic and capillary forces may be large enough to dominate the electrical behaviour of the material.

The resistivity of pore water is dominated by the concentration of ions in solution, the type of ions and the temperature. The presence of clay minerals strongly affects the resistivity of sediments and weathered rock. The clay minerals may be regarded as electrically conductive particles which can absorb and release ions and water molecules on its surface through an ion exchange process. Very roughly, igneous rocks have the highest resistivity, sedimentary rocks the lowest and metamorphic rocks intermediate. However, there is a considerable overlap. Resistivities of particular rock types vary with age and lithology, since the porosity of the rock and the salinity of the contained water are affected by both. For example the resistivity range of Precambrian volcanic is 200Ωm - 5000Ωm while for quaternary rocks of the same kind is 10Ωm - 200Ωm (Telford *et al*., 1976).

The mobility of ions increases with increasing temperature as the viscosity of water is lowered. Hence, a decrease in resistivity with increasing temperature can be observed for materials where electrolytic conduction dominates. A range of resistivities for different types of water is given in table 3.1.

Table 3.1: Electrical resistivity of some kinds of natural waters (ABEM instructional manual, LUND Imaging System).

TYPE OF WATER	**RESISTIVITY (Ωm)**
Precipitation	30 – 1000
Surface water in areas of igneous rock	30 – 500
Surface water in areas of sedimentary rock	10 – 100
Groundwater in areas of igneous rock	30 –150
Groundwater in areas of sedimentary rock	›1
Sea water	≈ 0.2
Drinking water (maximum salt content 0.25%)	› 1.8
Water for irrigation and livestock watering (max. salt content 0.25%)	› 0.65

3.7 RECONNAISSANCE SURVEY

Topographical maps and geological maps were obtained. A walk around the entire area to be surveyed with these maps was made, to consider whether resistivity surveying was suitable for the current research. It was discovered that the method was suitable. Therefore, possible profile lines were selected and the entire length of the planed profile lines inspected to ensure their practicability before returning to the area for the detailed survey.

3.8 INSTRUMENTATION AND FIELD PROCEDURE

The ABEM Lund imaging system was used for the data acquisition (see figure 3.5). It consists of:

ABEM Terrameter SAS4000;

ABEM Electrode Selector ES464, including connectors to Terrameter (serial port and current/voltage terminals);

ABEM SAS External Battery Adaptor (EBA) Reels of Cables and

Electrodes and Jumpers

For this research work, two reels of cables were used. The electrodes, numbering forty one were placed at intervals of 5m. However, the two innermost electrodes adjoining the two reels of cables coincided, thus yielding a total of 41 electrodes and a spread length of 200m. A total number of eight profiles were laid along the surface of the earth (Figure 1.2). The data obtained for each profile were processed using RES2DIVN software.

The modern field systems such as the Lund imaging system (Terrameter SAS4000) use a multicore cable to which 24 or more electrodes are connected at takeouts moulded on at predetermined equal intervals. Such a cable is very much like a seismic cable and is used in a similar way. The cable is connected to a switching module and to an earth resistance meter and



Figure 3.5. Picture of ABEM Lund Terrameter

computer through an RS232 port. With these systems, any electrodes may be switched to act as either current or potential electrodes and so within the constraints of the electrodes emplaced, any electrode arrangement can be employed. In practice either the two-electrode (pole-pole), Wenner, pole-dipole or dipole- dipole is employed.

The advent of automated data acquisition and inversion in recent years has increased the practical applicability of resistivity imaging tremendously. One of the new developments in recent years is the use of 2D electrical imaging surveys to map areas with moderately complex geology (Griffiths and Barker, 1993). Computer-controlled data acquisition systems generally consist of a resistivity instrument, a relay switching unit, a computer, electrode cables, various connectors and electrodes.

In the field survey, the multi-core cables are rolled out and electrodes are connected to it, after which the data acquisition software automatically checks the electrode contact and scans through a pre-defined measurement protocol.

2D resistivity imaging requires data to be recorded with many different electrode separations along a line. In this survey, the Wenner array with 5m interval between 41 electrodes was employed with each spread having a length of 200m. A laptop microcomputer together with an electronic switching unit is used to automatically select the relevant four electrodes for each measurement.

The typical setup for a 2-D resistivity survey with a number of electrodes along a straight line attached to a multi-core cable is shown in figure 3.6.

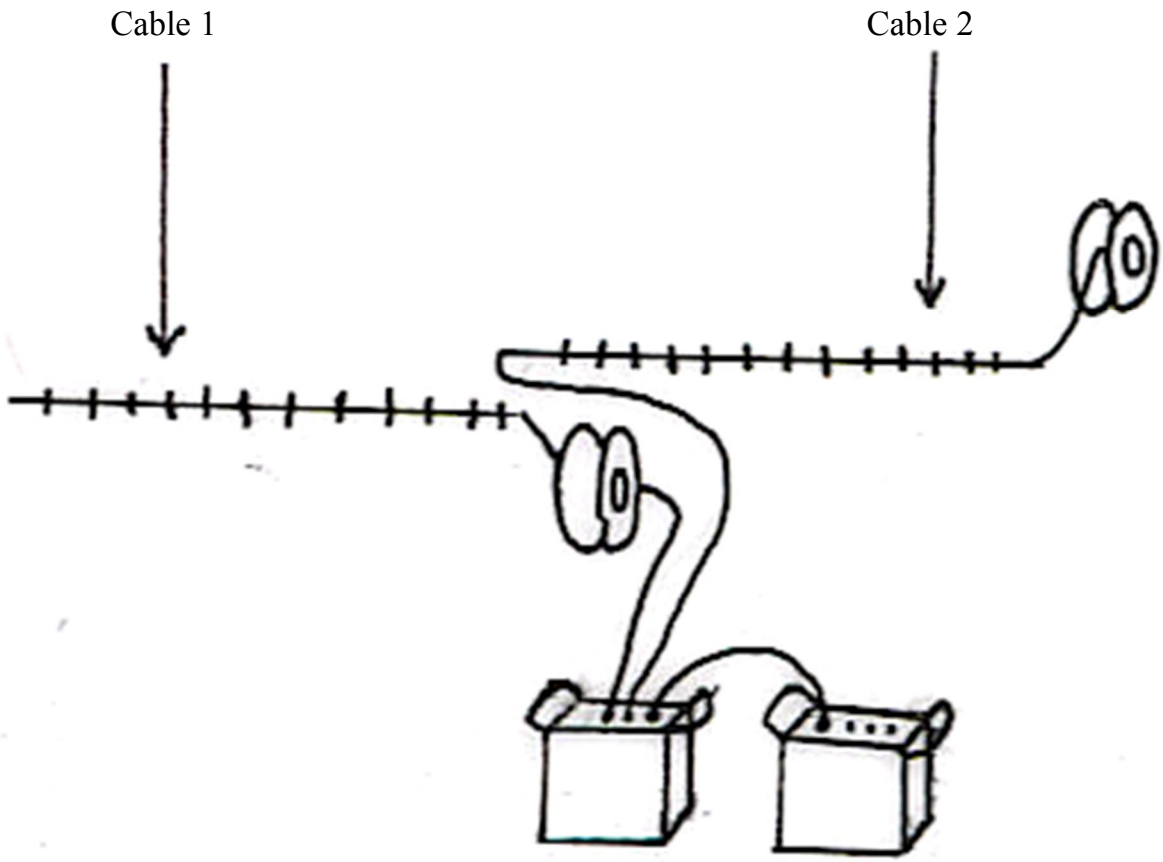


Fig. 3.6: Typical Electrode Layout of WEN32SX: Wenner CVES with two cables using the Terrameter SAS 4000 and ES464 in LUND Imaging. (ABEM Terrameter SAS4000/ SAS1000 instruction manual, 2006)

3.9 Electrode Arrays

Many configuration of electrodes have been designed (Loke, 1999). The choice of the best array for a field survey depends on the type of structure to be mapped, the sensitivity of the resistivity meter and the background noise level. In practice, the arrays that are most commonly used for 2-D imaging surveys are:

i) Wenner

ii) Dipole-Dipole

iii) Wenner-Schlumberger

iv) Pole-Pole

v) Pole-Dipole

Some of the characteristics of array that are considered for field survey are:

(i) The sensitivity of the array to vertical and horizontal changes in the subsurface resistivity.

(ii) The depth of investigation

(iii) The horizontal data coverage

(iv) The signal strength

(v) Sensitivity to surficial inhomogeneties

(vi) Electromagnetic coupling

3.9.1 Wenner Array

In the Wenner array the separation between adjacent electrodes is constant and the apparent resistivity ρ_a is given by:

$$\rho_a = 2\pi a \cdot \frac{\Delta V}{I} \quad \text{.....} \quad (3.21)$$

Where **"a"** is the uniform separation and **$2\pi a$** is the geometric factor.

The Wenner array is relatively sensitive to vertical changes in the subsurface resistivity below the centre of the array. However, it is less sensitive to horizontal changes in the subsurface resistivity. In general, the Wenner array is good in resolving vertical changes (i.e., horizontal structure), but relatively poor in detecting horizontal changes (i.e., narrow vertical structures). Among the common arrays, the Wenner array has the strongest signal strength. This can be an important factor if the survey is carried out in areas with high background noise. One disadvantage of this array for 2-D surveys is the relatively poor horizontal coverage as the electrode spacing is increased.

3.9.2 Dipole-Dipole Array

This array is widely used in resistivity/IP surveys because of the low Electromagnetic coupling between the current and potential circuits. The arrangement of the electrodes is shown in figure 3.7. The spacing between the current electrode pair, C_2 - C_1, is given as "a" which is the same as the distance between the potential electrode pair, P_1 - P_2. The factor "n" is the ratio of the distance between the C_1 and P_1 electrodes to the C_2 - C_1 or P_1 - P_2 dipole separation "a". For surveys with this array, the "a" spacing is initially kept fixed and the "n" factor is increased from 1 to 2 to 3 until up to about 6 in order to increase the depth of investigation.

The dipole-dipole array is very sensitive to horizontal changes in resistivity, but relatively insensitive to vertical changes in the resistivity. It is good in mapping vertical structures, such as dykes and cavities, but relatively poor in mapping horizontal structures such as sedimentary layers.

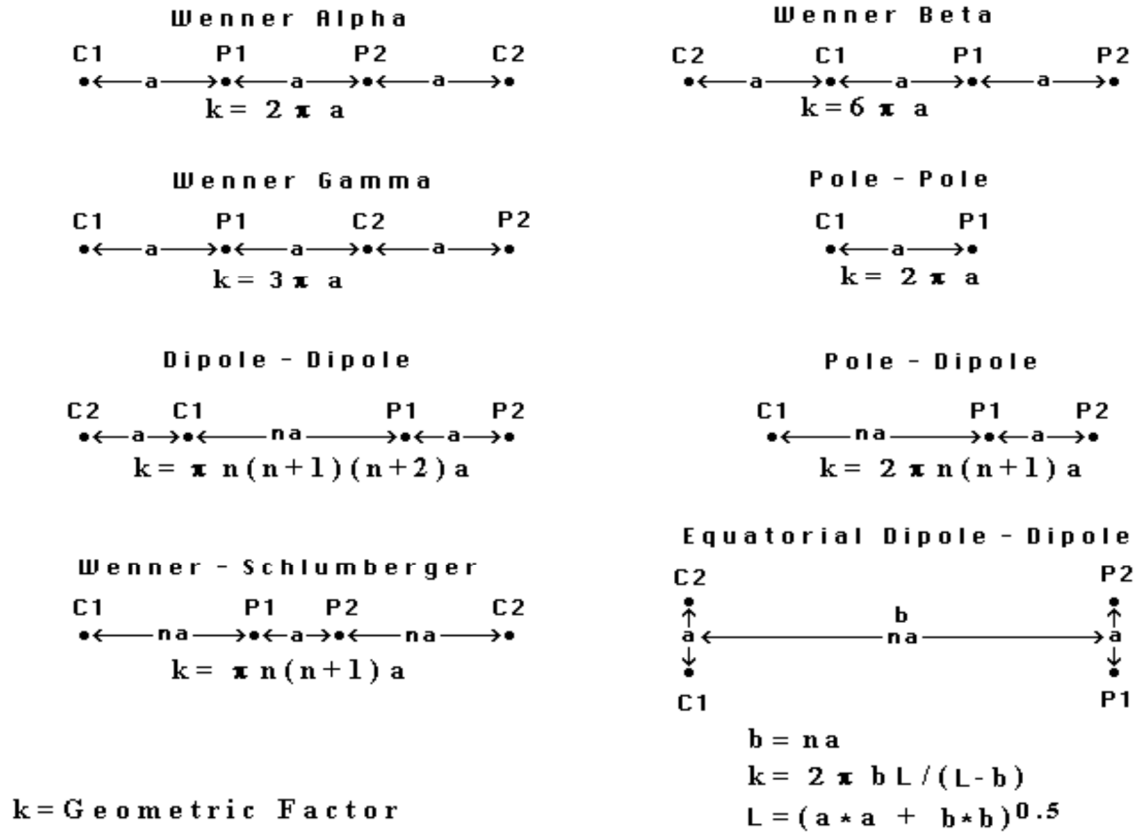


Figure 3.7: Common Arrays used in Resistivity Surveys and their Geometric Factors

The apparent resistivity, ρ_a is given by:

$$\rho_a = \pi n(n+1)(n+2)a.\frac{\Delta V}{I} \quad \text{..... (3.22)}$$

Where **"na"** is the distance between the two innermost electrodes (one current electrode and the next is potential electrode).

In general, this array has a shallower depth of investigation compared to the Wenner array. However, for 2-D surveys, this array has better horizontal data coverage than the Wenner. Another possible disadvantage of this array is the very small signal strength for large values of the "n" factor.

3.9.3 Wenner-Schlumberger Array

This is a new hybrid between the Wenner and Schlumberger arrays (Pazdirek and Blaha, 1996) arising out of relatively recent work with electrical imaging surveys. The array is moderately sensitive to both horizontal and vertical structures. In areas where both types of geological structures are expected, this array might be a good compromise between the Wenner and the dipole-dipole arrays. The signal strength for this array is smaller than that of the Wenner array but higher than the dipole-dipole array.

The Wenner-Schlumberger array has a slightly wider horizontal data coverage than the Wenner array, but narrower than that obtained with the dipole-dipole array.

The apparent resistivity, ρ_a , is given by:

$$\rho_a = \pi n(n+1)a\frac{\Delta V}{I} \quad \text{.....(3.23)}$$

Where "na" is the distance between the C_1 - P_1 or P_2 - C_2 electrodes. The "n" factor is the ratio of the distance between the C_1 - P_1 or P_2 - C_2 electrodes to the spacing between the P_1- P_2 potential pair.

3.9.4 Pole - Pole Array

This array is not as commonly used as the Wenner, dipole-dipole and Schlumberger arrays. In practice the ideal pole-pole array, with one current and one potential electrode does not exist. To approximate the pole-pole array, the second current and potential electrodes (C_2 and P_2) must be placed at a distance which is more than 20 times the maximum separation between C_1 and P_1 electrodes used in the survey. The effect of the C_2 or P_2 electrode is approximately proportional to the ratio of the C_1 - P_1 distance to the C_2 - P_1 distance. If the effects of the C_2 and P_2 electrodes are not taken into account, the distance of these electrodes from the survey line must be at least 20 times the largest C_1 - P_1 spacing used to ensure that the error is less than 5%. In surveys where the inter-electrode spacing along the survey line is more than a few metres, there might be practical problems in finding suitable locations for the C_2 and P_2 electrodes to satisfy this requirement.

Pole-pole array is popular in some applications such as archaeological surveys where small electrode spacings are used. It has the widest horizontal coverage and the deepest depth of investigation. However, it has the poorest resolution. Another disadvantage of this array is that because of the large distance between the P_1 and P_2 electrodes, it can pick up a large amount of telluric noise which can severely degrade the quality of the measurement.

The apparent resistivity $\boldsymbol{\rho_a}$ is given by:

$$\rho_a = 2\pi a.\frac{\Delta V}{I} \quad \text{.....} \quad (3.24)$$

Where **"a"** is the distance between C_1 and P_1 electrodes.

3.9.5 Pole-Dipole Array

The pole-dipole array also has relatively good horizontal coverage. It has a significantly higher signal compared with the dipole-dipole array and it is not as sensitive to telluric noise as the pole-pole array.

The pole-dipole array also requires a remote electrode, the C_2 electrode, which must be placed sufficiently far from the survey line. For the pole- dipole arrays, the effect of the C_2 electrode is approximately proportional to the square of ratio of the $C_1 - P_1$ distance to the C_2- P_1 distance. Thus the pole-dipole array is less affected by the C_2 remote electrode compared with the pole-pole array. If the distance of the C_2 electrode is more than 5 times the largest C_1 - P_1 distance used, the error caused by neglecting the effect of the C_2 electrode is less than 5%. The exact error also depends on the location of the P_2 electrode for the particular measurement and the subsurface resistivity distribution.

The signal strength is lower compared with the Wenner and Wenner-Schlumberger arrays but higher than the dipole-dipole array. For IP surveys, the higher signal strength (compared with the dipole-dipole array) combined with the lower EM coupling (compared with the Wenner and Wenner-Schlumberger Arrays) due to the separation of the circuitry of the current and potential electrodes makes this array an attractive alternative. The apparent resistivity ρ_a is given by:

$$\rho_a = 2\pi n(n+1)a\frac{\Delta V}{I} \quad \text{.....(3.25)}$$

Where "na" is the distance between C_1 and P_1 electrodes and "a" the distance between P_1 and P_2 electrodes.

3.10 The measurement Procedure for Wenner Electrode Configuration

For this research work Wenner electrode array was used since it is one of the most satisfactory arrays for imaging purposes (Griffiths and Barker, 1993). Wenner pseudo-sections have some advantages over dipole-dipole pseudo-section, the most important of which is that Wenner profiling data are less affected by near-surface resistivity variations which on dipole-dipole pseudo-sections can cause strong distortions of the contours.

Figure 3.8 shows the typical setup for a 2-D survey with a number of electrodes along a straight line attached to a multi-core cable.

Normally a constant spacing between adjacent electrodes is used. The multi-core cable is attached to an electronic switching unit which is connected to a laptop computer. The sequence of measurements to take, the type of array to use and other survey parameters are normally entered into a text file which can be read by a computer programme in a laptop computer. Different resistivity meters use different formats for the control file. After reading the control file, the computer programme then automatically selects the appropriate electrodes for each measurement.

In a typical survey, most of the field work is in laying out the cables and electrodes. After that, the measurements are taken automatically and stored in the computer. Most of the survey time is spent waiting for the resistivity meter to complete the set of measurements.

To obtain a good 2-D picture of the subsurface, the coverage of the measurements must be 2-D as well. As an example, figure 3.8 shows a possible sequence of measurements for the Wenner electrode array for a system with 20 electrodes. Here, measurement commences at one

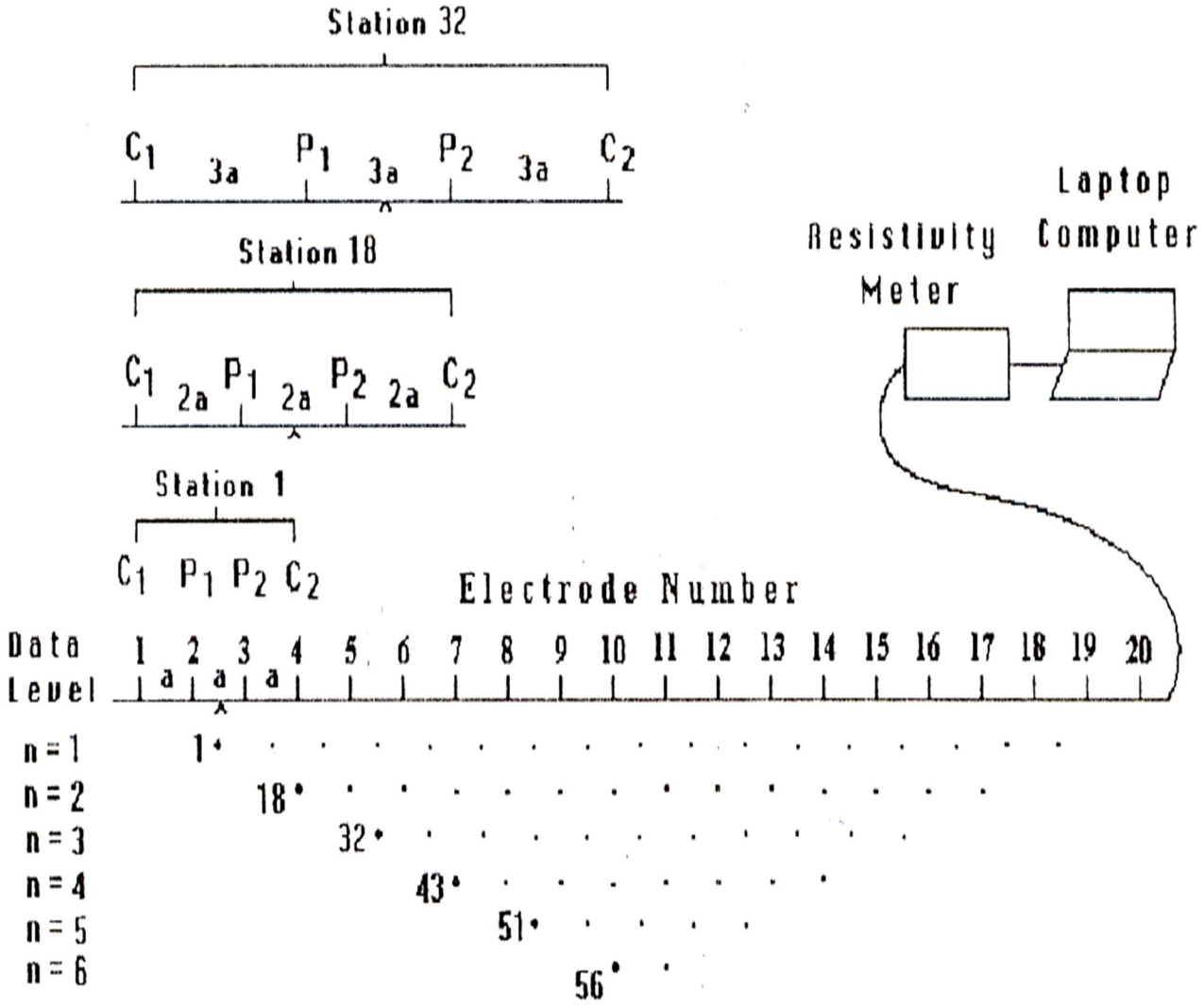


Figure 3.8 Principle for Building up a Pseudosection ***(ABEM Terrameter SAS4000/ SAS1000 instruction manual, 2006)***

end of the line using electrodes 1, 2, 3 and 4. The spacing between adjacent electrodes is "a". With Wenner array, the first step is to make all the possible measurements with electrode spacing of "a".

Electrode 1 is used as the first current electrode C_1, electrode 2 as the first potential electrode P_1, electrode 3 as the second potential electrode P_2 and electrode 4 as the second current electrode C_2. For the second measurement, electrodes 2, 3, 4 and 5 are used for C_1, P_1, P_2, and C_2 respectively. This is repeated down the line of electrodes until electrodes 17, 18, 19 and 20 are used for the last measurements with "a" spacing. The spacing is then doubled without moving on, the first active electrodes with "2a" electrode spacing being 1, 3, 5 and 7. For the second measurement, electrodes 2, 4, 6 and 8 are used. This process is repeated down the line until electrodes 14, 16, 18 and 20 are used for the last measurement with spacing "2a". The same process is repeated for measurements with "3a", "4a", "5a" and "6a" spacings and 200m. To get the best results, the measurements in a field survey should be carried out in a systematic manner so that, as far as possible, all the possible measurements are made. This will affect the quality of the interpretation model obtained from the inversion of the apparent resistivity measurements (Dahlin and Loke, 1998).

One technique used to extend horizontally the area covered by a survey, particularly for a system with a limited number of electrodes, is the roll-along method. After completing the sequence of measurements, the cable is moved past one end of the line by several unit electrode spacings.

CHAPTER FOUR

FIELD RESULTS AND INTERPRETATION

4.1 INTRODUCTION

As in all other geophysical methods, the interpretation of data from electrical imaging involves expressing in geological terms the information given by the measured apparent resistivity data. Such an interpretation demands, on the one hand, considerable practical experience with the method and, on the other hand, a sound knowledge of the geology of the region under consideration (Loke, 1999). In this work, all the available geological information on the project area was taken into consideration to constrain the interpretations.

4.2 DATA PROCESSING

The raw field data were processed using RES2DINV (Loke and Barker, 1996). This is a computer programme that automatically determines a two-dimensional (2-D) resistivity model for the subsurface for the data obtained from electrical survey. It is a Window based programme. This method is based on the following equation

$(\mathbf{J}^T\mathbf{J} + u\mathbf{F})\mathbf{d} = \mathbf{J}^T\mathbf{g}$

Where $\mathbf{F} = \mathbf{f}_x\mathbf{f}_x^T + \mathbf{f}_z\mathbf{f}_z^T$

$\mathbf{f}_x$ = horizontal flatness filter

$\mathbf{f}_z$ = vertical flatness filter

$\mathbf{J}$ = matrix of partial derivatives

u = damping factor

$\mathbf{d}$ = model perturbation factor

$\mathbf{g}$ = discrepancy vector

The *forward problem* is solved through a finite difference algorithm, whose main features are a versatile user-defined discretization of the domain and a new approach to the solution of the inverse Fourier transform. The forward modelling subroutine is used to calculate the apparent resistivity values. The *inverse procedure* is based on an iterative smoothness-constrained least-squares algorithm. This computer programme uses a smoothness constrained non-linear least-squares optimisation inversion technique to convert measured apparent resistivity values to true resistivity values and plot them as pseudosections.

The discrepancy vector, g, contains the difference between the calculated and measured apparent resistivity values. The magnitude of this vector is frequently given as a RMS (root-mean-squared) value. This is the quantity that inversion method seeks to reduce in an attempt to find a better model after each iteration. The model perturbation vector, d, is the change in the model resistivity values calculated using the above equation which normally results in an "improved" model. The above equation tries to minimize a combination of two quantities, the difference between the calculated and measured apparent resistivity values as well as the roughness (i.e., the reciprocal of the model smoothness) of the model resistivity values. The damping factor, u, controls the weight given to the model smoothness in the inversion process. The larger the damping factor, the smoother will be the model but the apparent resistivity RMS error will probably be larger.

One advantage of this method is that the damping factor and flatness filter can be adjusted to suit different types of data. The programme creates a resistivity cross-section, calculates the apparent resistivities for that cross-section, and compares the calculated apparent resistivities to the measured apparent resistivities. The iteration continues until a combined smoothness constrained objective function is minimized. The depth of investigation cannot be determined by simple calculations and it depends on the acquisition geometry, the conductivity

structures and data errors (Oldenburg and Li, 1999). However, they demonstrated through various modelling exercises that there is a loss of reliability in the inverted resistivity values at the bottom and ends of resistivity images where the resistivity values are least constrained by the data.

A common method for presentation of CVES and 2D resistivity data is the drawing of pseudosections. A pseudosection is made by plotting the data points in a diagram, using the length axis for the distance along the surveying line and the depth axis for the electrode separations, (ABEM LUND Instruction Manual, 2006), as indicated in (Figure 3.6). The distance for the electrode configuration midpoint is thus plotted against the electrode separation for each measured data point, letting the latter reflect the measurement depth. The corresponding apparent resistivities for the plotted points are then used to contour the variation in apparent resistivity along the surveying line. The pseudosection thus obtained reflects the variation of resistivity in the ground in a qualitative way, and approximate structures and depths to layer interfaces may be estimated. It should be noted that the pseudosection is simply a 2D equivalence of the plotted field data points on a linear depth scale. In this context, drawing of pseudosections needs computer assistance to be practicable due to the large amount of data.

The PSEUDO.EXE software and ERIGRAPH.EXE software are developed for automatic drawing of pseudosections in grey scales or colours, using linear interpolation between data points. Linear interpolation involves no smoothing of data, which gives a good indication of the data quality. Twelve different colours or grey levels are used for plotting data. Each data point used for drawing the pseudosection is indicated in the section by a dot. Presenting DC-resistivity data in colour plots may be disputable as the data do not contain any spectral information. However, presenting DC-resistivity data in colour plots makes it easier to see the variations in resistivity, which is important as small changes in resistivity in one part of a

long profile may be significant even if there is a very large variation along the profile. The selection of resistivity interval limit is of major importance when presenting data, as the perception of the plotted data is strongly controlled by the colours. A suitable selection of limits enhances the geological variation while unsuitable selection of limits may hide important information or enhance irrelevant features.

The programme was developed for plotting of DC-resistivity data measured with a multi-electrode array, implying electrode spacings are always an integer multiple of the smallest electrode spacing used. Furthermore, profile distance coordinates are assumed to fall into the same positions as data for the smallest electrode spacing or halfway between them. For long profiles the data matrix used for the interpolation routine will not be sufficient for plotting the whole profile at once. In cases where the data do not fit, it is automatically divided into small enough portions for the interpolation routine, and plotted one portion after the other in the same section. In this way there is no limit to the number of data points in the direction along the profile. There is however, a limit to the number of data points in the depth direction which depends on the array size specified before compiling the programme, but for DC-resistivity data the number of different electrode spacing is normally very limited.

The 2D model used by the programme divides the subsurface into a number of rectangular blocks, to determine the resistivity of the rectangular blocks that will provide an apparent resistivity pseudosection that agrees with the actual measurements. The arrangement of the blocks is loosely tied to the distribution of the data points in the pseudosection. The distribution and the size of the blocks are automatically generated by the programme, so that the number of blocks usually does not exceed the number of data points. The depth of the bottom row is set to be approximately equal to the equivalent to the depth of investigation of the data points with the largest electrode spacing (figure 4.1).

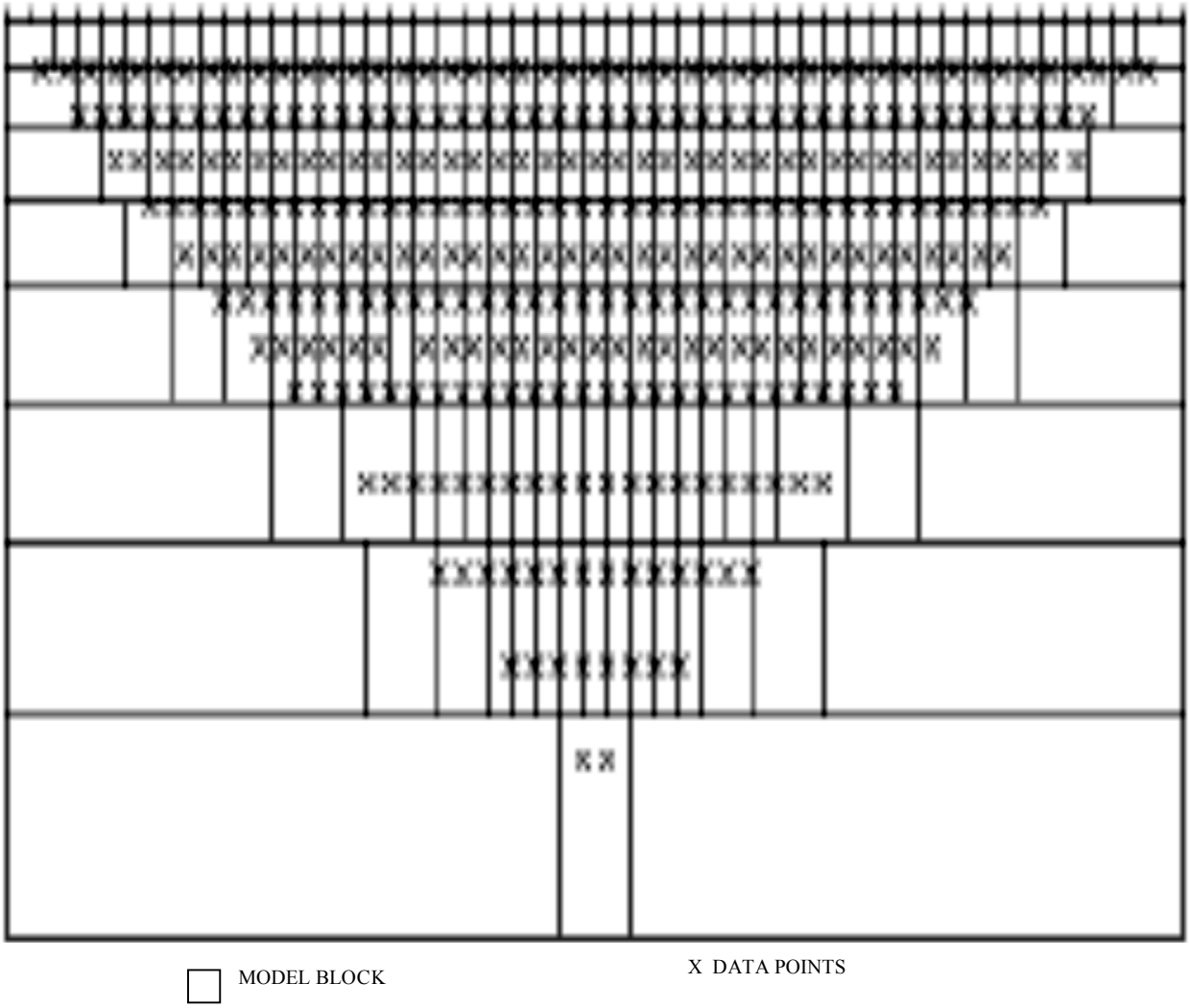


Figure 4.1 Arrangement of the blocks used in a model together with the data points in the pseudosection (RES2DINV ver.3.4).

The optimization method basically tries to reduce the difference between the calculated and measured apparent resistivity values by adjusting the resistivity of the model blocks. A measure of this difference is given by the root-mean-squared (RMS) error. However, the model with the lowest possible RMS error is usually chosen, but can sometimes show large and unrealistic variations in the model resistivity values and might not be the best model from a geological perspective. The most prudent approach is to choose the model at the iteration after which the RMS error does not change significantly.

4.3 INTERPRETATION TECHNIQUE

Interpreting the resistivity data consists of two steps: a physical interpretation of the measured data, resulting in a physical model, and a geological interpretation of the resulting physical parameters (Dahlin, 1996). The large-scale VES data are interpreted with the state-of-the-art interpretation technique, called the 2D smoothed damped least-squares inversion algorithm. The results obtained based on 2D inversion of field data and borehole information, were interpreted to determine the depth and extent of shallow bedrock, thickness of overburden, aquifer, *etc*. In interpreting LUND Imaging data, Computer assistance is needed due to the large amount of data collected from the field. The PSEUDO.EXE software and ERIGRAPH.EXE software for instance are developed for automatic drawing of pseudosections in grey scales or colour, using linear interpolating between data points. Third party software packages for resistivity data processing can also be used for advanced interpretation. One example of such a programme is RES2DINV.EXE, which performs smoothness constrained inversion (automatic model interpretation) using finite difference forward modelling and quasi-Newton techniques (Loke, 1999). The true resistivity structure was interpreted using automatic 2D smoothness constrained least squares inversion. The smoothness constrain prevents unstable and extreme

solutions, whereas a quasi-Newton reduces the numerical calculations (Loke and Barker, 1996). Quite often a useful amount of information can be extracted from a pseudosection by careful inspection of the contour pattern and apparent resistivity values, particularly if some geological control is available. Contours tend to follow horizontal or gently sloping boundaries between strata of different resistivities, though steep contacts are much smoothened. Such steep boundaries, provided they show a strong resistivity contrast, can be identified using some of the gradient measure. Contour peaks and troughs are correctly positioned relative to the subsurface features giving rise to them, and some estimate of depths at which boundaries occur may be made. Hence, qualitatively speaking, the subsurface structure may be quite obvious though this is by no means always so. If there are marked departures from 'two-dimensionality', the contour pattern may be affected by resistivity contrasts close to, but outside the plane of the section. Such effects can lead to serious errors both at the qualitative and quantitative stages of interpretation. Even if the acquisition of a data set is straightforward due to the improvements in resistivity measuring devices, the interpretation involves many factors and can be difficult when some parameters in the inversion procedure are neglected. Such parameters include the stability, robustness and uniqueness of the inversion algorithm (Cardarelli and Fischanger, 2006).

4.4 GEOLOGIC SECTION FROM BOREHOLE DATA

Boreholes are necessary and reliable source of primary data, and electrical resistivity imaging interpretations provide secondary information. Although borehole data provide a good sample for a six-inch diameter of a vertical cylindrical volume, it can be a poor representation of the several square metres surrounding the borehole. Alternatively, electrical resistivity imaging (ERI) provides block averages of resistivity. Also, borehole data are far more expensive to acquire than the data from an ERI survey.

The 2D inversion results of the present ERI survey were correlated with the lithology information obtained from a borehole at Administrative Area in the study area. This geological well-log (Figure 4.2) determined by Belmont Nigeria Limited, Kaduna(Drilling Engineers, 2001), shows that the topsoil in the study area is lateritic consisting of clayey, silty and brownish material which may be up to 10.0m thick in the area. The layer below this is about 5.0m thick. These two layers overlie the partially weathered schist rock. The section shows that, at the depth of 35.0m, fresh basement rock was encountered.

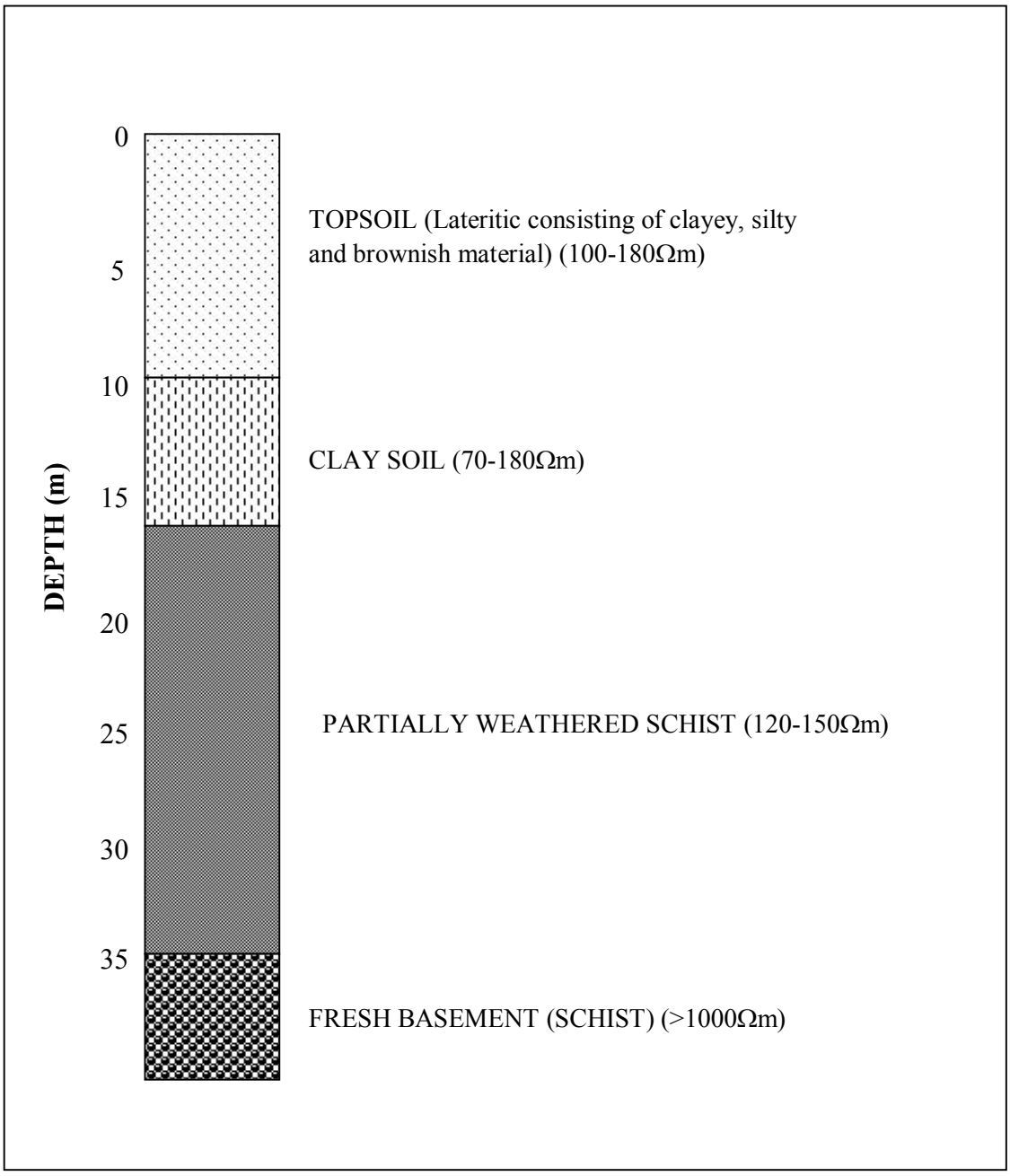


Figure 4.2 Geological Well-Log obtained from Belmont Nigeria Limited, Kaduna (Drilling Engineers, 2001).

4.5 TYPICAL RESISTIVITY VALUES FROM PREVIOUS WORKS

Resistivity values obtained from previous works close to the study area were used to correlate the results of the present survey, and these are considered in this section. Representative resistivity values of earth materials in the study area were derived from the works of Ososami (1968) and that of Messrs Preussag Ltd as contained in Olufemi (1985). These values were compared with the result of Baimba (1978) and Okwueze (1978) who also worked in different basement areas of Kaduna State. From these works and the resistivity values of various types of earth materials suggested by other authors, the representative resistivity values presented in Table 4.1 were compiled as a guide for the present work.

Based on the general representative resistivity values and the geological control (borehole log) discussed above, the resistivity values shown in Table 4.2 were used for the interpretation of the results of this present work.

Table 4.1: Typical Resistivity values compiled from previous works: Baimba (1978); Shemang (1990); Aminudeen (1990); Hassan *et al.,* (1991) and Ameloko (2006).

ROCK TYPES	RESISTIVITY VALUES(Ωm)
Clay-fresh water	30 – 70
Fadama loam	30 – 90
Dry clay	40 – 100
Weathered basement	20 – 100
Clay, schist and sand (topsoil)	100 – 200
Sand and Grave	100 – 180
Weathered laterite	200 – 500
Slightly weathered basement	200 – 500
Fresh laterite	500 – 600
Dry sand	500 – 1000
Fresh basement (crystalline)	>1000

Table 4.2: Resistivity Values Adopted for this present Work

ROCK TYPES	RESISTIVITY RANGES(Ωm)
Clay	1 – 120
Sand, gravel and lateritic soil	100 – 180
Weathered basement	20 – 400
Fractured basement	135 – 900
Weathered laterite	500 – 1000
Fresh basement	>1000

4.6 INTERPRETATION OF THE RESULTS

A good knowledge and use of the geology of an area are very important for any meaningful interpretation of any geophysical data collected from the area. Therefore, in this work, information obtained from previous works and borehole log within the area of survey was taken into consideration in arriving at the interpretations.

4.6.1 Profile One

Figure 4.3 shows the resistivity inversion results with 4 iterations and 7.4% total average RMS error for profile 1. This shows measured apparent resistivity pseudosection, the calculated apparent resistivity pseudosection and the inverse model resistivity section of profile one, but with colour infill instead of line contours. These data have been inverted to produce the image of figure 4.3c. The electrical image has revealed two layers, namely the top soil which is reddish brown laterite and the fractured/weathered basement. The near surface material shows the presence of clay with resistivity values ranging from about 26Ωm-44Ωm and thickness of about 7.0m. The low resistivity values of the layer shows that the rock material is saturated with water, since the resistivity of rock decreases as the percentage of water saturation increases. The colour layers show that weathered basement is fractured. The weathered basement has a range of resistivity of 44Ωm-170Ωm with a thickness of 22.3m.

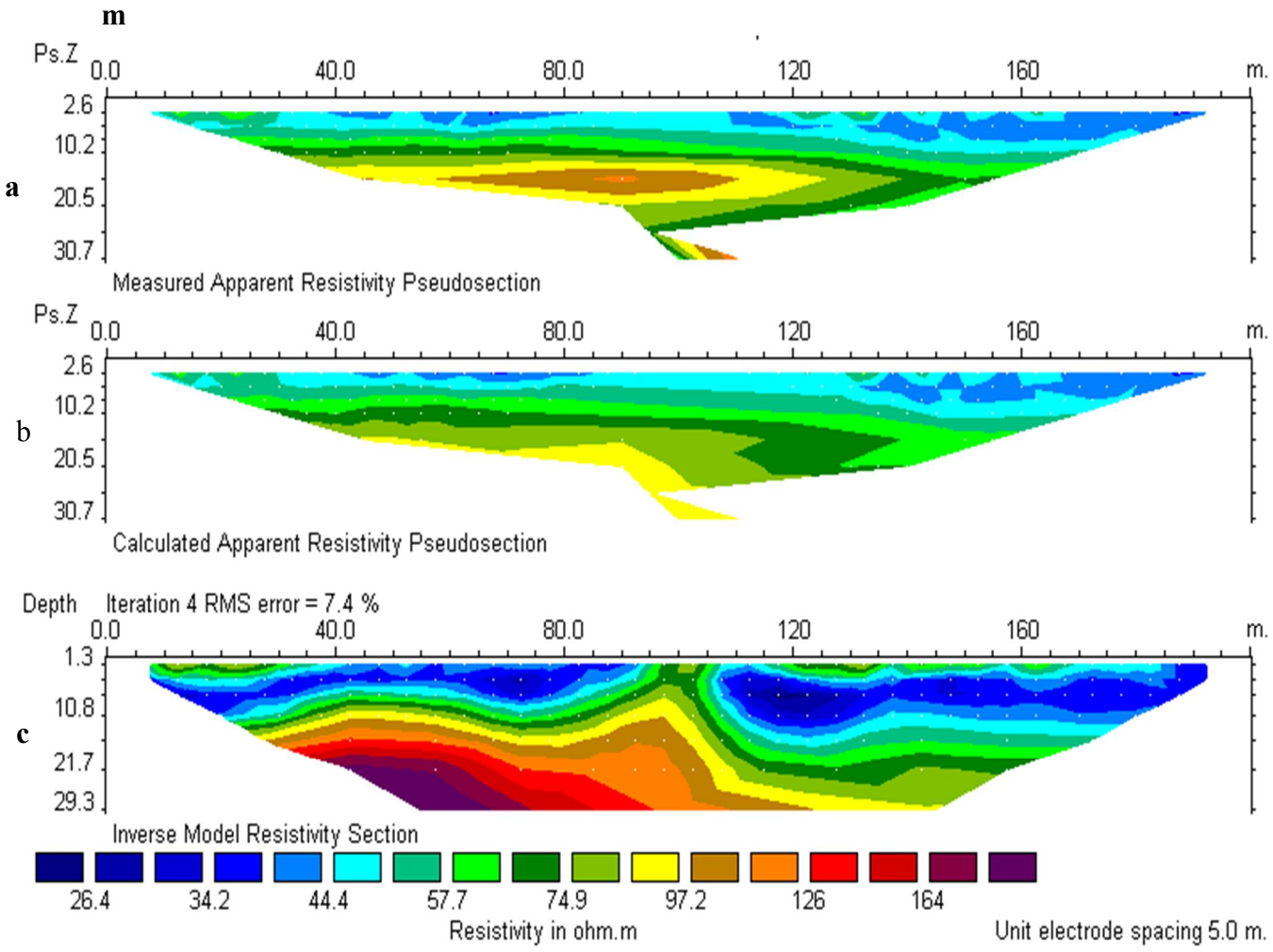


Figure 4.3. Electrical image along profile 1, (a) observed data plotted as a coloured pseudosection; Ps.Z = pseudo-depth, (b) the pseudosection computed from the model and (c) the image or model showing true depth and true formation resistivity.

4.6.2 Profile Two

Figure 4.4 shows the resistivity inversion results with 4 iterations and 7.8% total average RMS error for profile 2. This shows measured apparent resistivity pseudosection, the calculated apparent resistivity pseudosection and the inverse model resistivity section of profile 2.

A careful look at the electrical image of this profile shows intercalation of sandy and lateritic clay as the top soil with the thickness of about 7.0m and resistivity values ranging from 40Ωm to about 65Ωm. This corresponds with the resistivity table (table 4.2) used as a guide. Underlaying the topsoil is the weathered basement from the depth of about 7.0m to about 29.3m with resistivity values ranging from about 80Ωm to 220Ωm. The low value of the resistivity is a clear indication that the basement is highly fractured. The thickness of the weathered basement is 22.3m.

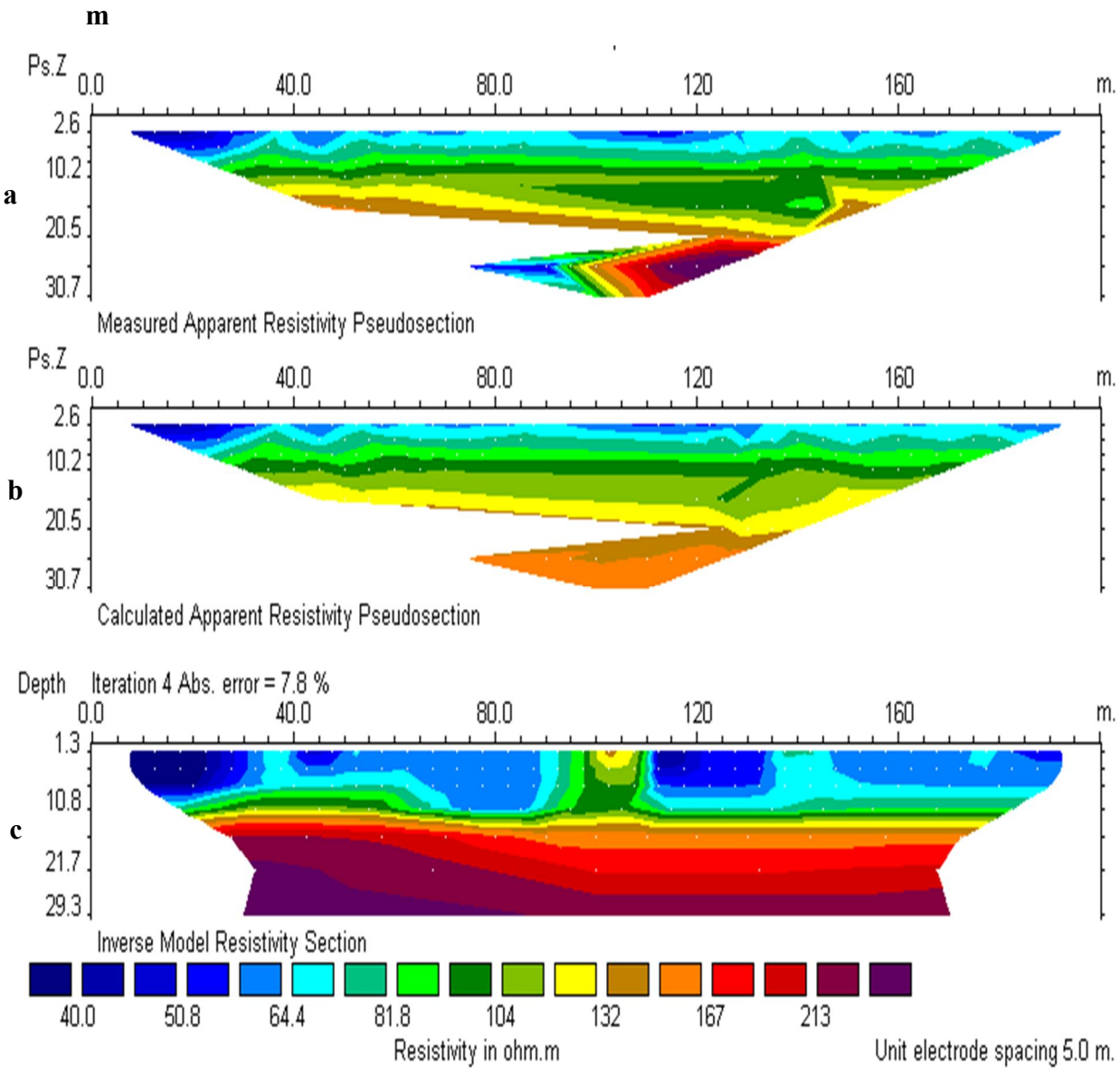


Figure 4.4. Electrical image along profile 2, (a) observed data plotted as a coloured pseudosection; Ps.Z = pseudo-depth, (b) the pseudosection computed from the model and (c) the image or model showing true depth and true formation resistivity.

4.6.3 Profile Three

Figure 4.5 shows the resistivity inversion results (iteration 9, 32.1% total average RMS error) for profile 3. The top layer is composed of consolidated laterite, gravel, sand, silt and clay having a high resistivity range of 400Ωm - 1400Ωm. This is the first layer (topsoil) with a thickness of about 7.0m. The weathered bedrock clearly shows on the image immediately underneath the topsoil with a resistivity range of about 30Ωm - 470Ωm with a thickness of about 22.3m. It is made up of clay, sand and other weathered rock materials. Between 105m – 125m marks a low resistivity (32Ωm - 100Ωm) section is observed rising to the surface. This is probably clayey soil or groundwater trapped in the aquifer streaming to the surface. Patches of high resistivity material are observed between 65.0m – 80.0m, 90.0m – 95.0m, 135.0m – 140.0m and at 160.0m and 185.0m marks with resistivity greater than 1376Ωm and are probably a hard crystalline rocks or possibly core-stones or unweathered bedrock at depths between 13m and 10.8m. The fresh basement is not shown by the image and is believed to occur at greater than 29.3m depth.

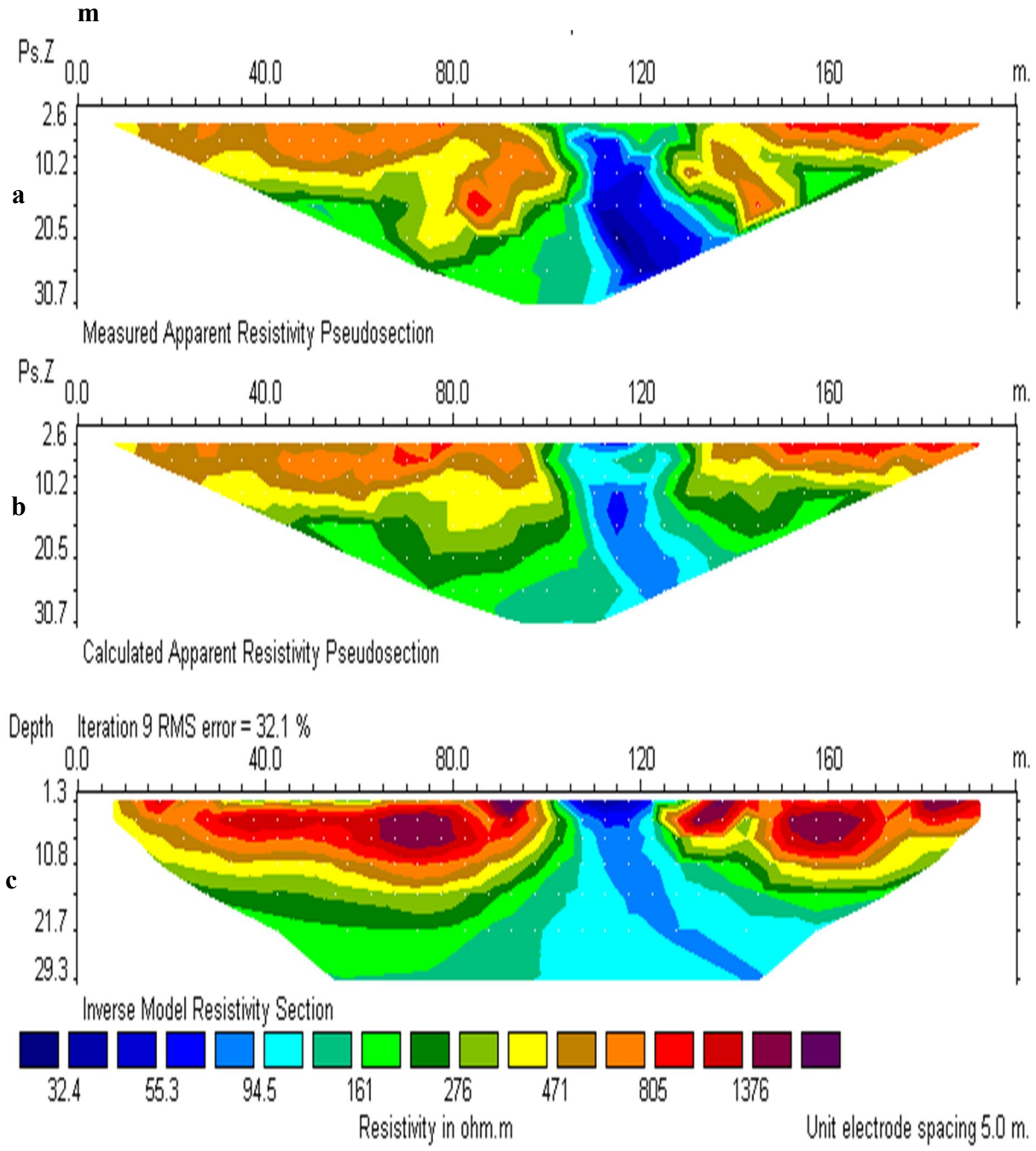


Figure 4.5. Electrical image along profile 3, (a) observed data plotted as a coloured pseudosection; Ps.Z = pseudo-depth, (b) the pseudosection computed from the model and (c) the image or model showing true depth and true formation resistivity.

4.6.4 Profile Four

Figure 4.6 shows the resistivity inversion results (iteration 5, with 3.5% total average RMS error) for profile 4. High resistivity (270Ωm - ›2435Ωm) weathered materials of thickness about 15.0m and composed of consolidated laterite, gravel, sandy clay and silt overlay low resistivity (‹52Ωm - 471Ωm) aquifer zone at a depth of 21.7m. Patches of unweathered bedrock (›2435Ωm), embedded in the consolidated laterite, clearly occur at 25m - 45m, 85m – 95m and 160m – 172m marks close to the surface, at a depth above 10.0m. The increased thickness of weathering here provides a good reservoir with a higher probability of bedrock fracturing. The estimated thickness of the weathered basement (aquifer zone) is 22.3m. The fresh basement is not shown by the image and is believed to occur at greater than 29.3m depth.

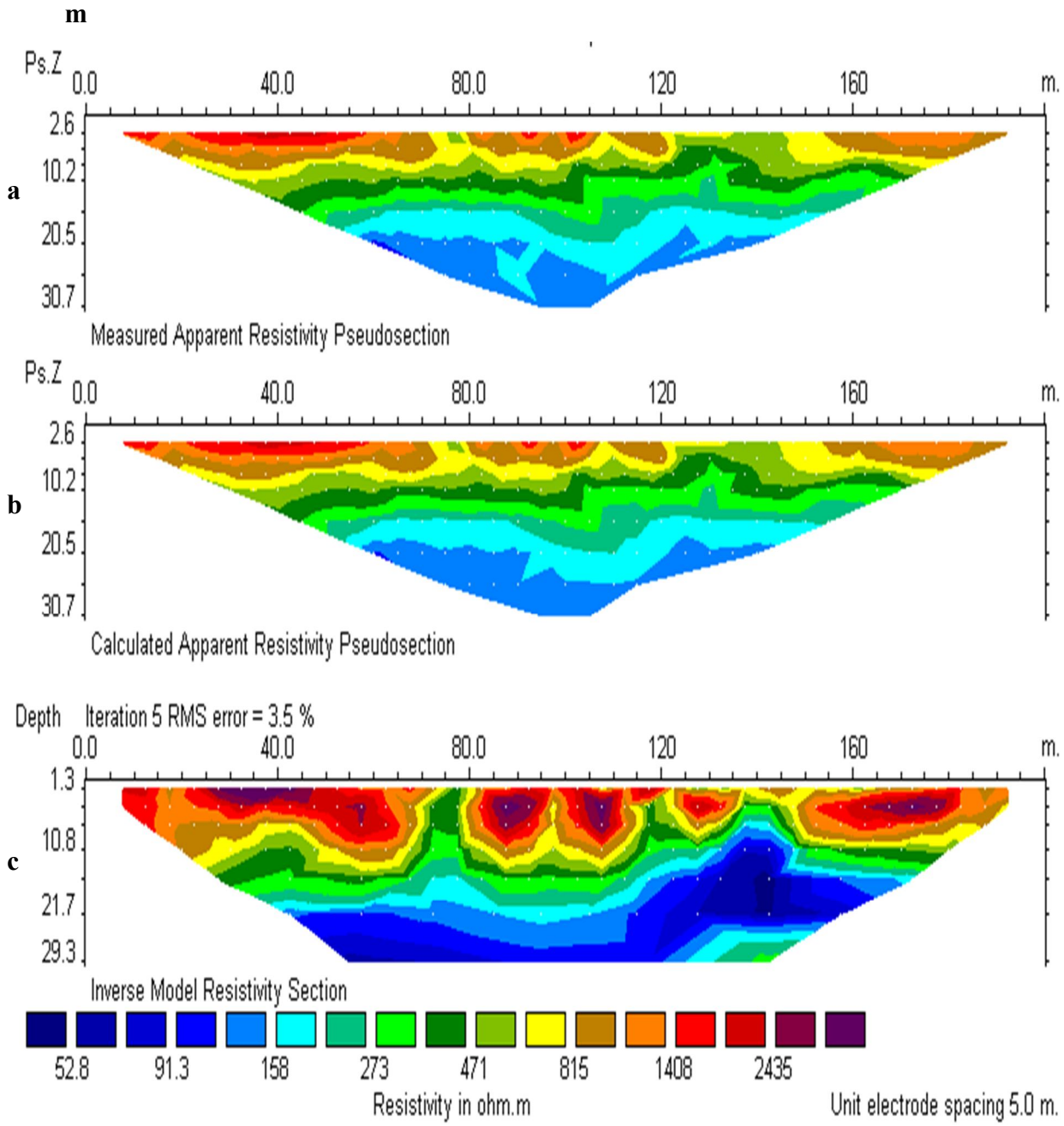


Figure 4.6. Electrical image along profile 4, (a) observed data plotted as a coloured pseudosection; Ps.Z = pseudo-depth, (b) the pseudosection computed from the model and (c) the image or model showing true depth and true formation resistivity.

4.6.5 Profile Five

Figure 4.7 shows resistivity inversion results with 10 iterations, and 10.7% total average RMS error for profile 5. A thin layer of resistivity anomaly greater than 800Ωm on the top of the topsoil indicates the presence of consolidated laterite sandwiched in gravel and sand. The weathered basement starts from the depth of about 5.0m to the fresh basement. The weathered basement shows variable resistivity (<6.52Ωm - 204Ωm) signifying fractured crystalline rock which has weathered into clay, sand and gravel and constituting the aquifer. Also a very low resistivity section is seen in this image at the depth of 29.3m at 140m mark. It is suspected to be a clay or trapped groundwater. The fresh basement is not revealed in this image, so it is likely to be at a depth greater than 29.3m.

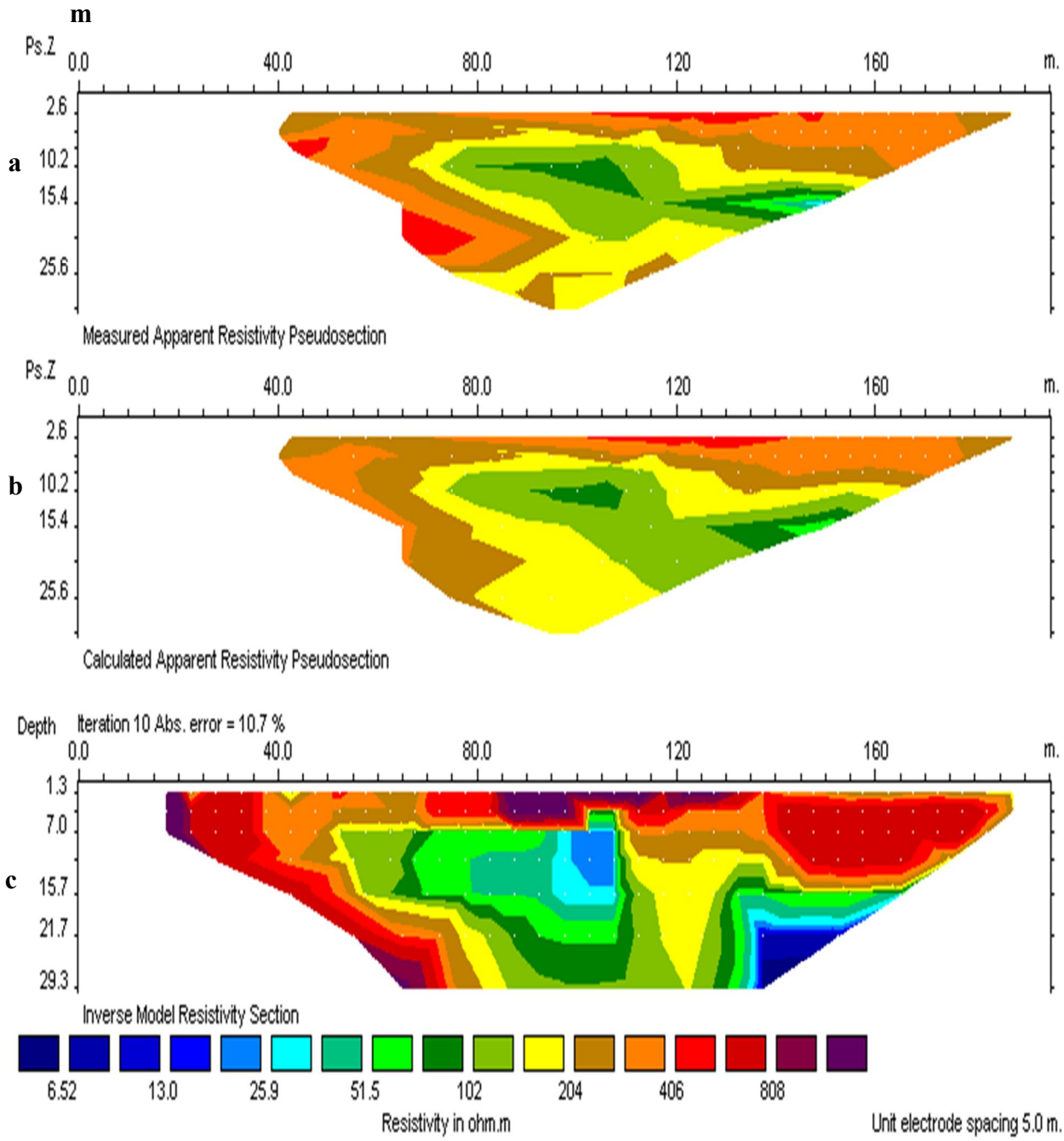


Figure 4.7. Electrical image along profile 5, (a) observed data plotted as a coloured pseudosection; Ps.Z = pseudo-depth, (b) the pseudosection computed from the model and(c) the image or model showing true depth and true formation resistivity.

4.6.6 Profile Six

Figure 4.8 shows the electrical image of profile 6 with 4 iterations and 6.8% total average RMS error. Two layers of close resistivity values can clearly be identified in this section.

The first layer which is a mixture of lateritic clay and sandy clay extends from the surface to a depth of about 7.0m with the resistivity values ranging from less than 20Ωm to about 63Ωm. These low resistivity values show that the materials in this layer are saturated with water. The immediate layer extends from about 7.0m to fresh basement. This section is believed to be a weathered basement with resistivity values ranging from 63Ωm to about 100Ωm is believed to be clay material. This weathered basement is severely fractured.

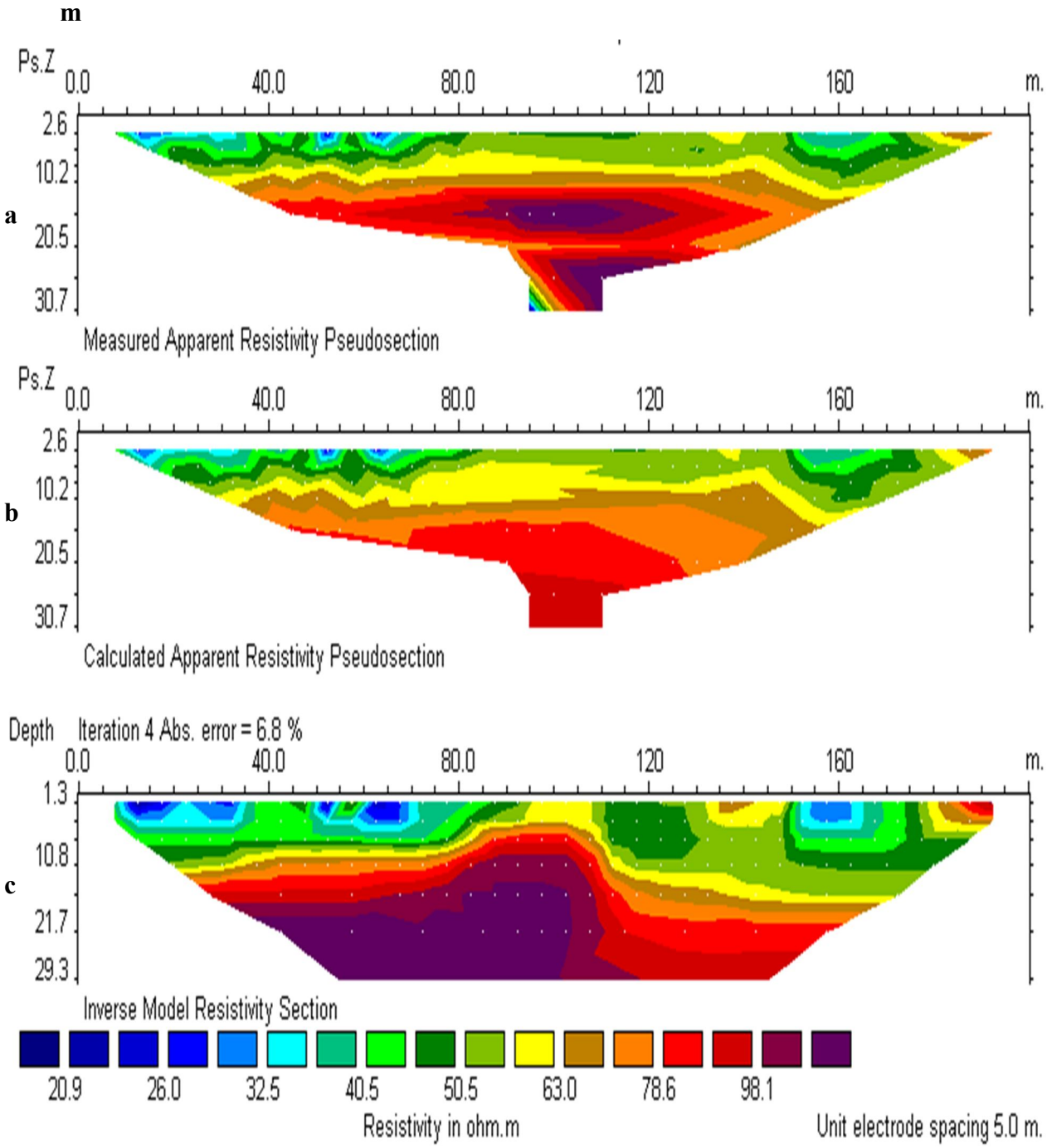


Figure 4.8. Electrical image along profile 6, (a) observed data plotted as a coloured pseudosection; Ps.Z = pseudo-depth, (b) the pseudosection computed from the model and(c) the image or model showing true depth and true formation resistivity.

4.6.7 Profile Seven

Figure 4.9 shows the resistivity inversion results with 4 iterations with 4.0% total average RMS error for profile 7. This shows measured apparent resistivity pseudosection, the calculated apparent resistivity pseudosection and the inverse model resistivity section of profile 7. The inverse model resistivity section reveals low resistivity (19Ωm - 50Ωm) materials near the surface. It is clear from the geology of the area based on borehole information that the near-surface material is an intercalation of lateritic clay and sandy clay. Directly underlaying these materials is the weathered basement with resistivity values ranging from about 40Ωm - >68Ωm. The low resistivity value of the bottom layer is a clear indication that the basement is severely fractured. The weathered basement extends from about 5m to the fresh basement.

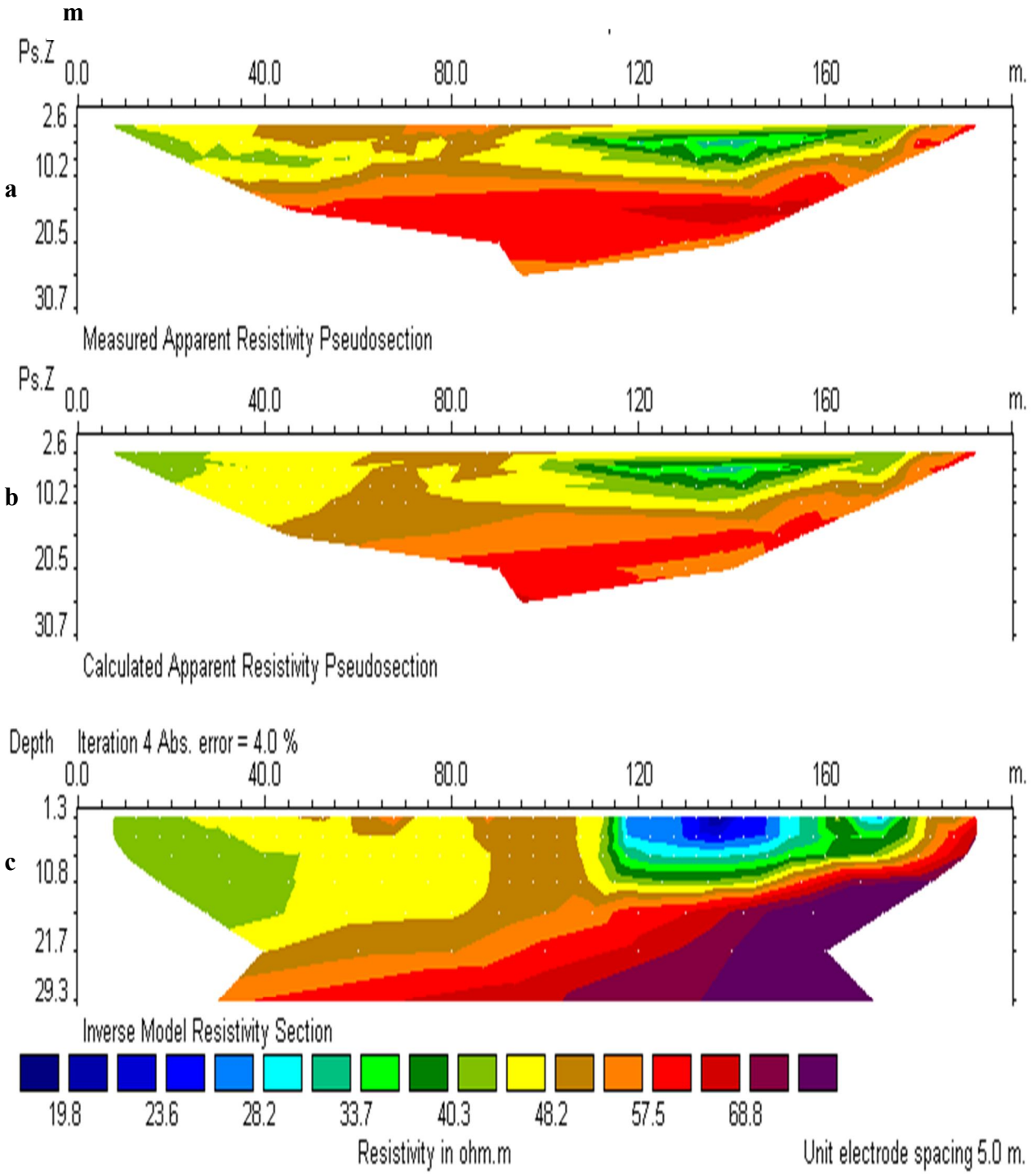


Figure 4.9. Electrical image along profile 7, (a) observed data plotted as a coloured pseudosection; Ps.Z = pseudo-depth, (b) the pseudosection computed from the model and(c) the image or model showing true depth and true formation resistivity.

4.6.8 Profile Eight

Figure 4.10 shows the resistivity inversion results with 6 iterations with 6.1% total average RMS error for profile 8. This shows measured apparent resistivity pseudosection, the calculated apparent resistivity pseudosection and the inverse model resistivity section of profile 8. The inverse model resistivity section clearly reveals two layers with an anomaly of high resistivity value of (>1461Ωm), which is believed to be a boulder. The top soil with resistivity values between 28Ωm and 50Ωm is a clay material with thickness of about 7.0m. While the bottom layer has resistivity values between 49.9Ωm and 832Ωm and thickness of about 22.3m, which is the weathered basement.

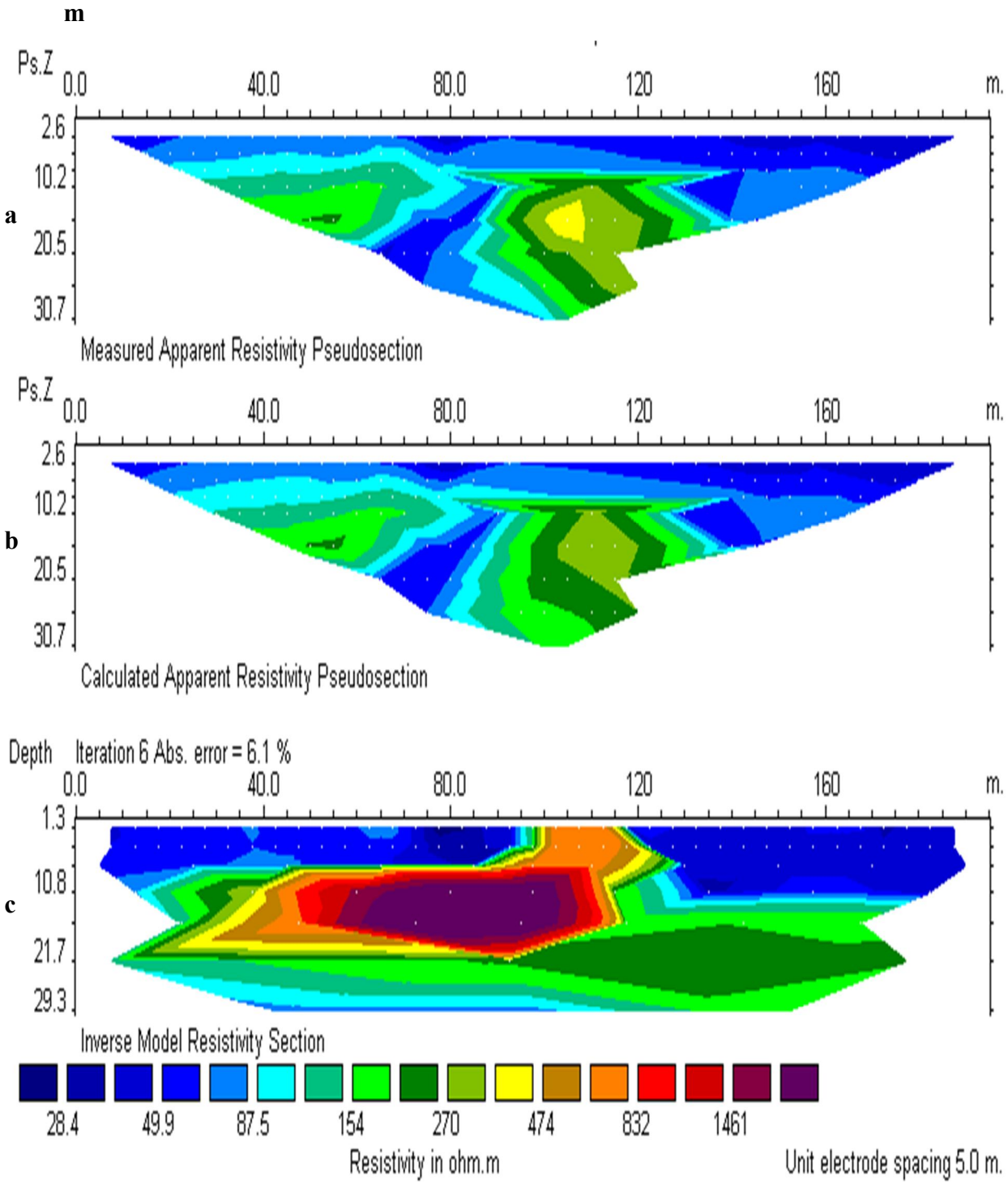


Figure 4.10. Electrical image along profile 8, (a) observed data plotted as a coloured pseudosection; Ps.Z = pseudo-depth, (b) the pseudosection computed from the model and(c) the image or model showing true depth and true formation resistivity.

4.7 GENERAL INTERPRETATION OF THE RESULTS

4.7.1 Variation in thickness of the Weathered Basement

The thickest portion as indicated by figure 4.11 of the weathered basement is about 22.0m which is around the profiles 1, 5, 7 and 8 and the thinnest portion is about 15.0m. The parameters of investigation have helped in identifying potential positions for the siting of boreholes; the points with the thickest portion of weathered basement of about 22.0m are good aquifers for boreholes. This is because the weathered basement is the fractured or aquiferous zone characterized by structural elements like fissures, cracks, faults, etc. that enhance groundwater storage and permeability. For engineering work, the bedrock always serves as pillar support to the civil engineering structures, but it is not revealed by any profile so the depth to the bedrock is not ascertained. Area with the shallow depths to the bedrock could be the best for any high-rise buildings.

4.7.2 Isoresistivity Map

The isoresistivity map (figure 4.12) has helped to show at a glance the resistivity distributions over the whole area at preferred depth of 10.8m. The map reveals different resistivity zones which constitute two diagnostic layers, the topsoil and the weathered basement resulting from the disintegrated schistose rock materials. The resistivity variation on the map is an indication that the study area has a good potential for groundwater exploration. The resistivities of subsurface are generally influenced by the fluid situation or degree of saturation. Therefore areas with low resistivity values obtained sometimes may indicate abundance of moisture or presence of clay. Extremely low resistivity values are usually associated with presence of saline water at the subsurface. The resistivity values of the surface are high as a result of the laterite disseminated

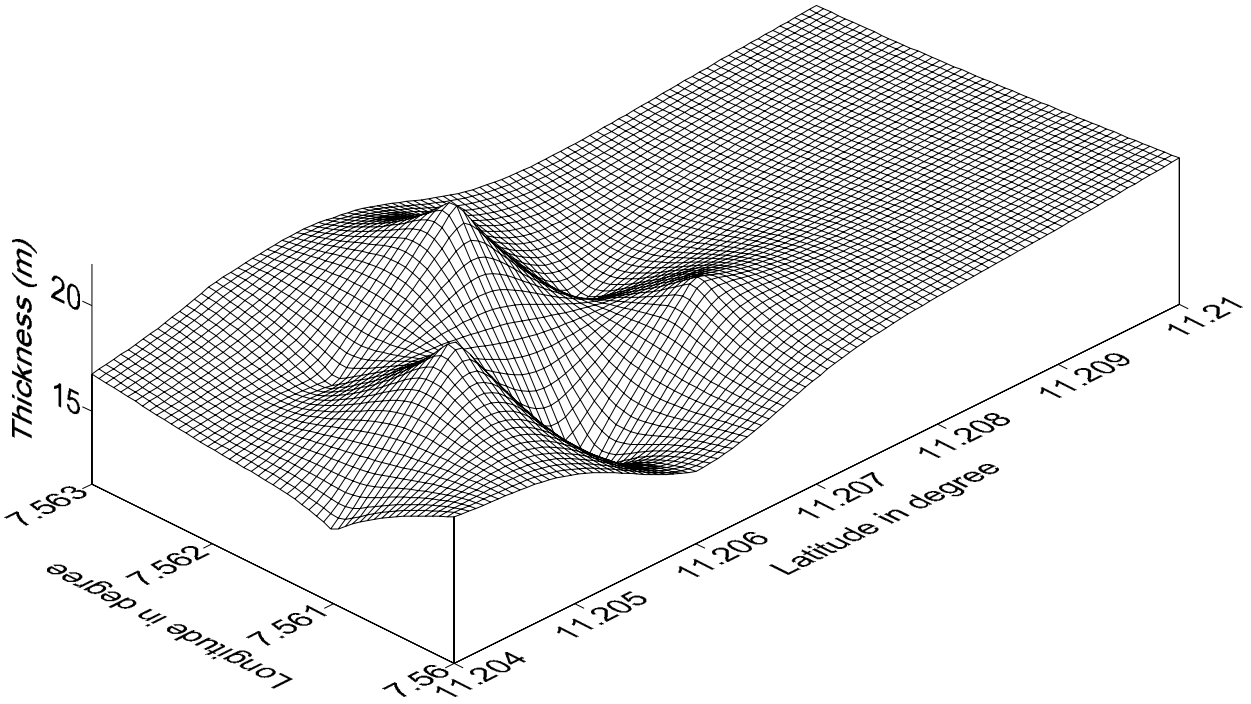


Figure 4.11 Surface Plot of the Weathered Basement Map of the Research Area

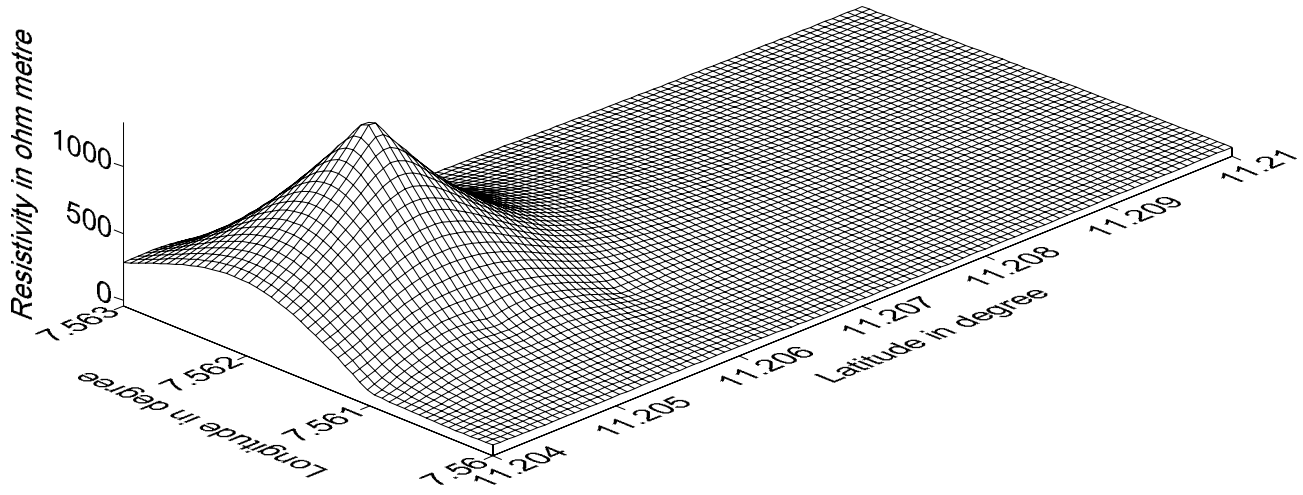


Figure 4.12 Isoresistivity Map of the Research Area

around the study area. The topsoil constitutes the layer within which normal civil engineering foundation is founded. This layer is composed of sandy clay, clay, sand and laterite. Engineering competence of the topsoil can be qualitatively evaluated from the resistivity. The higher the resistivity value, the higher the competence of the layer. Also, laterite is most competent of the delineated topsoil as indicated on the profiles 3, 4 and 5. For purpose of engineering work, area of very low resistivity values as indicated by profiles 1, 2, 6, 7 and 8 which suggest presence of clay, need to be excavated and filled with laterite which drain water quickly.

CHAPTER FIVE

DISCUSSION OF RESULTS, CONCLUSIONS AND RECOMMENDATIONS

5.1 DISCUSSION OF RESULTS

The models obtained from 2D inversion of the field data using different starting models mainly showed that the inversion algorithm is stable. After that, comparison of the measured apparent resistivity pseudosection and the calculated apparent resistivity pseudosection resulted in a reasonably good agreement with the inverse model resistivity section. As a result, this demonstrates the stability of the 2D inversion algorithm to give reliable models. Based on the electrical images obtained in the study area, the following deductions are made.

5.1.1 Basement

The depth to the basement is not revealed by this investigation because of the length of the spread used. The study reveals different resistivity zones which constitute two distinct layers. These two layers are the topsoil and the weathered basement. They both constitute the overburden.

1. The topsoil: the topmost of which is about 5.0m thick to 7.0m and is composed of reddish brown lateritic clay with resistivity ranges of 20Ωm-400Ωm.

2. The weathered basement: the topsoil is immediately underlain by the weathered basement which consists of disintegrated schistose rock materials, sand and gravel. This layer has a relatively low resistivity due to the presence of water, so this layer is regarded as the aquifer, because it can usually hold water. Also, the layer is highly weathered and the degree of weathering increases towards the fresh basement. This increased thickness of bedrock weathering is a proof of the capability of this layer to provide a good water reservoir with a high probability of the presence of fractures in the weathered basement. The average thickness and

resistivity of this layer are about 22.8m and 30-470Ωm respectively. This correlates well with the 20.0m thickness provided by the borehole log within the study area.

3. The fresh bedrock: the fresh basement rock was not revealed due to the length of the spread used. The maximum depth of probe, which is 29.3m, is not up to the depth of 35.0m to the fresh basement as indicated by the borehole log.

5.1.2 Groundwater potentials

Groundwater modeling is a rapidly evolving field in hydrology. Groundwater systems can be simulated, allowing predictions to be made about the effects of aquifer exploitation on water quantity and water quality. The reliability of the results of such numerical model studies largely depends upon the available parameter data that are fed into the model, and their precision. The electrical images reveal large thicknesses of weathered materials overlaying the basement rocks. The increased thickness of weathering provides a good water reservoir with a high probability of bedrock fracturing (Acworth, 1987). These form the aquifer in the study area. To site successful boreholes to tap groundwater in hard rock or basement terrains is a complex problem because of the heterogeneous nature of the aquifer system. But as fractures do not constitute a significant volume of the rock, fractured basement has low porosity.

For this reason a good borehole providing long term high yields is one which penetrates a large thickness of regolith, which acts as a reservoir and also intersects fractures in the underlying bedrock, the fractures providing the rapid transport mechanism from the reservoir and hence the high yield. Boreholes which intersect fractures, but which are not overlain by thick saturated regolith, cannot be expected to provide high yield in the expected long term. A borehole which penetrates saturated regolith but which finds no fractures in the bedrock is likely to provide sufficient yield for a hand pump only. However, only electrical methods can provide data on water quality, which is one of the reasons why they have become so successful in

groundwater exploration. Considering the resistivity inversion model as well as topographic, geologic and hydrogeological implications, groundwater potential of the NAPRI site could be considered as reasonably encouraging for borehole development.

5.1.3 Subsurface engineering evaluation of the study area

The geologic sequence beneath the study area is composed of topsoil, weathered layer, partly weathered/fractured basement and the fresh bedrock. The topsoil constitutes the layer within which normal civil engineering formation is founded. This layer is composed of sandy clay, clay, sand and laterite.

The topsoil is generally clayey with resistivity values between 20-400Ωm. The sub-grade which is the weathered basement has low resistivity values between 30-470Ωm. This indicates the accumulation of groundwater within the weathered basement, and possibly suggests that the layer is made of clay which is not permeable and hence does not drain water quickly. Engineering competence of the topsoil can be qualitatively evaluated from the layer resistivity. The higher the layer resistivity value, the higher the competence of the layer.

The resistivities of subsurface are mostly influenced by the degree of fluid situation and the chemistry (or salinity) i.e. quality of saturating fluid. Low resistivity values obtained from field measurements sometimes may indicate abundance of moisture. Extremely low values are usually associated with presence of saline water within the earth medium. Due to high ion exchange capacity of clay minerals, they are also associated with low resistivity field readings. In the study area (NAPRI), the resistivities of upper geologic layers of profiles 3, 4 and 5 are generally high due to lateritic cover.

The earth medium acts as a natural filter to percolating fluid. Its ability to retard and filter percolating fluid is a measure of its protective capacity. The protective capacity of an overburden overlying an aquifer is proportional to its hydraulic conductivity (Henriet, 1976).

But high clay content generally corresponds with low resistivities and low hydraulic conductivities. Hence, the protective capacity of the overburden can be considered as being proportional to the longitudinal unit conductance (S) defined as the ratio of the overburden thickness to its resistivity. The higher the overburden longitudinal conductance, the higher is the protective capacity.

Soil corrosivity which can lead to severe corrosion failure is known to be associated with low resistivity. Low electrical resistivity is an indication of good electrical conducting paths arising from reduced aeration, increased electrolyte saturation or high concentration of dissolved salts in soil. Soil resistivity can therefore be classified in terms of the degree of soil corrosivity.

5.2 CONCLUSIONS

The major goal of this research was to study the subsurface structure of NAPRI environment in Shika. In connection with this goal, the survey was carried out to determine the thickness of the overburden, weathered basement, depth to the aquifer and to identify the weak zones that are proned to subsidence and the competent zones that can support massive engineering structures.

Eight profiles were taken along the surface of the ground and electrical imaging was carried out along the lines. Electrical images provide a more detailed view of subsurface structure than can be obtained using other geophysical techniques and may therefore lead to a better understanding of the fracturing system.

The inversion result of profile one reveals two distinct layers ranging from lateritic clay topsoil to fractured basement. The low resistivity value of the layers is an indication that the materials are saturated with water. The electrical image of profile two shows intercalation of lateritic clay and sandy clay as near-surface material with relatively thick weathered basement.

The basement is fractured as clearly indicated by its low resistivity values (about 213Ωm). The resistivity inversion results for profile three, four and five also revealed that the near-surface material is not uniform. They show that the weathered basement is highly fractured. Their high resistivity values at the surface indicate the presence of lateritic soil which was seen in the field. The resistivity inversion result for profile six also reveals that the near-surface material is not uniform. It shows that the weathered basement is highly fractured. This is evident from the low resistivity value (about 98Ωm) of the basement. The depth to the weathered basement from the surface ranges from 5.0m at the beginning of the profile to about 7.0m towards the end of the profile. The resistivity inversion result of profile seven also indicates that the near-surface is not uniform. The weathered basement is severely fractured as revealed by the low resistivity (about 68Ωm) of the basement. The resistivity inversion result of profile eight shows an anomaly with high resistivity value (about 1500Ωm) which may likely be a boulder, underlain by a weathered basement with relatively low resistivity value (about 270Ωm).

Mostly, the electrical images of the profiles show two distinct layers, the topsoil and the weathered basement. The resistivity values of these layers indicate that the materials are saturated with water. None of the electrical images shows fresh basement. The maximum depth of investigation achieved is 29.3m. This indicates that the fresh basement is deeper than 29.3m from the surface which agrees with the borehole lithology within the study area. Thus, the minimum overburden thickness of the area is 29.3m as revealed by the results (pseudosections). The results also revealed that the basement rock is highly fractured and the fracturing decreases with depth.

The depth to the aquifer is believed to be the same with the depth to the weathered basement which ranges from 5.0m to 7.0m. The thickness of the aquifer cannot be ascertained because the study could not reveal the depth to the fresh basement.

5.3. RECOMMENDATIONS

The electrical imaging technique is not a reconnaissance tool. It is suitable for the detailed study of problem areas that have been selected using other techniques, such as Electromagnetic Method (EM) or resistivity traversing. But to obtain the best results in the future, a combination of this results and wider spread greater than 200m is suggested.

Two-dimensional electrical surveys should be used in conjunction with seismic or GPR surveys as they provide complementary information about the subsurface.

As a fundamental and important subsurface investigation tool, geophysical measurements should be utilized before any geotechnical constructions design process. This will help to identify areas which are liable to possess structural defects during and after the construction and necessary precaution(s) will be included in the design/construction plan. This would reduce the amount of money wasted daily in the rehabilitation and reconstruction of failed structures.

Areas where large deposit of clay or subsurface formations that are likely to weather into clay are delineated, such areas should be excavated and filled with materials which allow quick drainage of water, such as quartzite and laterite.

Finally, future work should be extended beyond the limits of the profiles traversed in this work for better understanding of the study area, and also the roll-along CVES surveying method of probing the subsurface should be employed to give a better coverage at depth. 3D resistivity survey should be undertaken in the survey area.

REFERENCES

ABEM Instruction Manual, (2006). ABEM Instrument AB, Terrameter SAS4000/SAS1000 LUND Imaging System.

Acworth, R. I., (1987). *The development of crystalline basement aquifers in a tropical environment. Quarterly Journal of Engineering Geology*, 20, 265-272.

Adamu, A. G., (1973). Basement geology of Zaria, Samaru Area. An Unpublished B.Sc. project, Geology Department, Ahmadu Bello University, Zaria.

Akpoborie, I. A., (1972). Hydrogeological Control of Structures along Samaru Creek. Unpublished M.Sc. Thesis, Department of Physics, Ahmadu Bello University, Zaria.

Ameloko, A.A., (2006). Two-dimensional Imaging over the western part of the Kubanni River Basin, Zaria, Nigeria. An unpublished M.Sc. Thesis, Department of Physics, Ahmadu Bello University, Zaria.

Aminudeen, A. I., (1990). Geoelectrical investigations for groundwater in four villages in RoniLocal Government Area, Kano State, Nigeria. Unpublished M.Sc. Thesis, Department of Physics, Ahmadu Bello University, Zaria.

Baimba, A. B., (1978). Resistivity and refraction seismic methods for groundwater exploration at Zango, Kaduna state. Unpublished M. Sc. Thesis, Department of Physics, Ahmadu Bello University, Zaria.

Barker, R. D., (1989). Depth of investigation of a generalized collinear 4-Electrode array. Geophysics, 54, 1031 – 1037.

Belmont, (2001). Nigeria Engineering Drilling Company Limited. K7 College Road, Kurmin Mashi, Kaduna, Kaduna State.

Cardarelli, E. and Fischanger, F., (2006). 2D data modelling by electrical resistivity tomography for complex subsurface geology. *Geophysical Prospecting*, 54,121 – 133.

Clark, N. J., (1960). Elements of petroleum reservoirs: SPE of AIME. Vol. 23, p8.

Chiemeke, C. C. and Osazuwa, I. B., (2007). Applications of seismic refraction tomography for subsurface imaging in central Northern Nigeria; Nigeria Journal of physics. Vol. 16, pp1-8.

Dahlin, T., (1996). 2D resistivity surveying for environmental and engineering applications. *First Break,* 14 (7), 275-283.

Dahlin, T. and Loke, M. H., (1998). Resolution of 2D Wenner Resistivity Imaging as assessed by numerical modelling, Journal of Applied Geophysics, 38, 237-249.

Edwards, L.S., (1977). A modified Pseudosection for Resistivity and Induced Polarization. Geophysics, 42, 1020 – 1036.

Eigbefo, C., (1978). Hydrogeology of the Kubanni Drainage basin, Zaria. Unpublished M. Sc. Thesis, Department of Physics, Ahmadu Bello University, Zaria.

Farouq, A. U., (2001). Geoelectric investigation of the groundwater potential in the Institute for Agricultural Research Farm, Zaria. Unpublished M.Sc. Thesis, Department of Physics, Ahmadu Bello University, Zaria.

Grant, N. K., (1969). The late Precambrian to early Paleozoic Pan African Orogeny in Ghana, Togo, Dohomey and Nigeria. Geol. Soc. Am. Bull., Vol. 80, pp. 45-56.

Griffiths, D. H. and Barker, R. D., (1993). Two-dimensional resistivity imaging and modeling in areas of complex geology. *Journal of Applied Geophysics,* Vol. 29, Pp 211-226.

Hassan, M., Ajayi, C. O. and Ojo, S. B., (1991). A Basement structure determined from Geoelectric mapping of the Kubanni River Basin, Zaria. *Nigerian Journal of Physics,* Vol. 3, pp. 166-173.

Henriet, J.P., (1976). Direct application of the Dar Zarrouk parameters in groundwater surveys. *Geophysical prospecting,* Vol. 24, pp. 23-26.

Joda, F.O., (1990). The establishment of a local gravity network for Zaria area. Unpublished M.Sc. Thesis, Department of Physics, Ahmadu Bello University, Zaria.

Kearey, P. and Brooks, M., (1988). An Introduction to Geophysical Exploration. Blackwell Scientific Publication, London.

Keller, G. V. and Frischknecht, F. C., (1966). Electrical methods in geophysical prospecting. Pergamon Press.

Koefoed, O., (1979). Geosounding Principles, 1: Resistivity sounding measurements. Elsevier press.

Loke, M. H., (1999). Electrical imaging surveys for environmental and engineering studies; a practical guide to 2-D and 3-D surveys. Self Published Note Book, 15-57.

Loke, M. H. and Barker R. D., (1996). Rapid least-squares inversion of apparent resistivity pseudosections using a quasi-Newton method. Geophysical Prospecting, 44, 131 – 152.

McCurry, P., (1970). The geology of Degree Sheet 21, Zaria. Unpublished M.Sc. Thesis, Department of Geology, Ahmadu Bello University, Zaria.

McCurry, P., (1976). The geology of the Precambrian to Lower Paleozoic rocks of Northwestern Nigeria. A review in Kogbe, C.A. (Ed), *Geology of Nigeria*. Elizabethan Publishing Company, Lagos, Pages 15-39.

Ojo O. F., (2007). Two Dimensional electrical imaging of the subsurface structure of Bomo dam, Zaria. Unpublished M.Sc. Thesis, Department of Physics, Ahmadu Bello University, Zaria.

Okwueze, E. E., (1978). Geophysical exploration for groundwater in Kankarg, Kaduna State. Unpublished M. Sc. Thesis, Department of Physics, Ahmadu Bello University, Zaria.

Oldenburg, D.W. and Li, Y., (1999). Estimating depth of investigation in D.C. Resistivity and IP surveys. *Geophysics*, 64 (2), 403-416.

Olowu, D., (1967). Preliminary investigations of the groundwater conditions in Zaria, sheet 102 SW: *Geological Survey of Nigeria, Report* No. 1462.

Olufemi, R. O., (1985). Hydrogeology of Jama'a Kubanni Area, (Zaria Sheet 102 SW). Unpublished B. Sc. Project, Department of Geology, Ahmadu Bello University, Zaria.

Osasami, I. A., (1968). Assessment of the groundwater in the Kubanni Valley. Unpublished M.Sc. Thesis, Department of Physics, Ahmadu Bello University, Zaria.

Oyewoye, M. O., (1964). Geology of the Nigerian Basement Complex, *Journal of Nigerian Mining,* Geological and Metallurgical Society, Vol. 1, pp. 87-102.

Pazdirek, O. and Blaha, V., (1996). Examples of resistivity imaging using ME-100 resistivity field acquisition system. 58th Conference and Technical Exhibition Extended abstracts, Amsterdam. pp 5-20.

Russ, W., (1957). The geology of parts of Niger, Zaria and Sokoto provinces with special reference to the occurrence of gold. *Geological Survey* of Nigeria, Bulletin. No. 27, p42.

Shemang E. M., (1990). Electrical depth soundings at selected well sites within the Kubanni River Basin, Zaria, Unpublished M.Sc. Thesis, Dept. of Physics, Ahmadu Bello University, Zaria.

Telford, W. M., Geldart, L. P., Sheriff, R.E. and Keys, D.A., (1976): Applied Geophysics. Cambridge University Press, London, 860pp.

Tokarski, A., (1972). Heterogeneous Terrace Arrangement West of Ahmadu Bello University, Zaria. Occasional paper No. 1, Department of Geology, Ahmadu Bello University, Zaria, p42.

Truswell, J. F. and Cope, R. N., (1963). The geology of parts of Niger and Zaria provinces, northern Nigeria. *Geography Society of Nigeria. Bulletin* 29, 52pp.

Ward, S. H., (1990). Resistivity and induced polarization methods; in geotechnical and environmental geophysics; Edited by S. H. Ward. *Society of Exploration Geophysicists (SEG),* Tulsa, Okla., vol.1, pages 147-189.

Wright, J. B. and McCurry, P. (1970). The geological map of the Zaria area; in Zaria and its region edited by M. J. Mortimore, Department of Geography, Ahmadu Bello University, Zaria; Occasional paper, No. 4, pp 5-12.